Nano-Enhanced Therapeutic Potential of Moringa oleifera: Hepato- and Nephroprotective effects of Green- Synthesized Silver Nanoparticles in CCl 4 - Induced toxicity

Usama Bin Matloob Abbasi

abbasiusama329@gmail.com

Pir Mehr Ali Shah Arid Agriculture University

Imtiaz Ahmad Khan

Pir Mehr Ali Shah Arid Agriculture University

Zaman Javed

Pir Mehr Ali Shah Arid Agriculture University

Muhammad Akram

Pir Mehr Ali Shah Arid Agriculture University

Rahmatullah Qureshi

Pir Mehr Ali Shah Arid Agriculture University

Hafiz Muhammad Hashim Qayyum

Pir Mehr Ali Shah Arid Agriculture University

Article

Keywords: Moringa oleifera, Drug Delivery, Silver Nanoparticles, Antioxidant, Phytomedicine

Posted Date: May 18th, 2026

DOI: https://doi.org/10.21203/rs.3.rs-9492124/v1

Additional Declarations: No competing interests reported.

Nano-Enhanced Therapeutic Potential of *Moringa oleifera*: Hepato- and Nephroprotective effects of Green-Synthesized Silver Nanoparticles in CCl_4-Induced toxicity

Authors:

Usama Bin Matloob Abbasi[1] (abbasiusama329@gmail.com) **ORCID iD:** 0009-0007-8769-981X

Prof. Imtiaz Ahmad Khan[1](imtiazarana@uaar.edu.pk)

Zaman Javed[1] (zamanjaved896@gmail.com)

Muhammad Akram[1]dr.m.akram@uaar.edu.pk

Prof. Dr. Ramatullah Qureshi[2] (rahmadtullahg@uaar.edu.pk)

Hafiz Muhammad Hashim Qayyum[1] (hmhq007@gmail.com)

Corresponding Authors:

Usama Bin MatloobAbbasi (abbasiusama329@gmail.com) **ORCID iD:** 0009-0007-8769-981X

Prof. Imtiaz Ahmad Khan(imtiazarana@uaar.edu.pk)

Affiliation:

[1] Department of Veterinary Pathology, Faculty of Veterinary and Animal Sciences, PMAS-Arid Agriculture University Rawalpindi, Pakistan

[2]Department of Botany, PMAS-Arid Agriculture University Rawalpindi, Pakistan

Abstract

Background: Exposure to environmental toxins and xenobiotics is a major contributor to oxidative stress-mediated liver and kidney injury and remains a major global concern. *Moringa oleifera,* also known as miracle tree, has demonstrated significant hepatoprotective and nephroprotective effects due to its potent antioxidant and anti-inflammatory properties. However, limitations associated with poor bioavailability can reduce the overall effectiveness of *Moringa oleifera.*

Purpose: The present study evaluated the hepatoprotective and nephroprotective potential of *M. oleifera* leaf extract and its green-synthesized silver nanoparticles (MO-AgNPs) against CCl_4-induced toxicity in Wistar rats.

Methods: Silver nanoparticles were synthesized by using aqueous leaves extract and characterized by UV-Vis spectroscopy, FTIR, SEM, EDX and XRD, confirming their crystalline nature and successful formation. The synthesized AgNPs had an average diameter of 43 nm. Eighty-four rats were divided into seven groups (n=12): Group-I (Control), Group-II (CCl_4), Group-III (CCl_4+ Silymarin @ 100 mg /kg body weight), Group-IV (CCl_4 +*Moringa oleifera* leaves extract @ 300 mg/ kg body weight), Group-V (CCl_4+*Moringa oleifera* leaves extract @ 500 mg/ kg body weight), Group-VI(CCl_4+Ag-NPs @ 2.5 mg/kg body weight), and Group-VII (CCl4 + Ag-NPs @ 4 mg/kg body weight). DPPH and H_2O_2 antioxidant scavenging activity were assessed to check the antioxidant potential of *Moringa oleifera* crude extract and Ag-NPs. Blood samples were collected after 24 hours after the last administration i.e. at day 30 and serum was extracted for liver function tests, renal function tests, and total proteins concentration. Histopathology of liver and kidney were performed for histoarchitectural evaluation.

Results: TheCCl_4-treated group showed significant increases in liver and kidney biomarkers along with a decrease in total proteins concentration and severe histoarchitectural damage, demonstrating induction of toxicity in all groups. Treatment with *Moringa oleifera* crude extract and its Ag-NPs ameliorated the damage in a dose-dependent manner; however MO-AgNPs @ 4mg/kg and *Moringa oleifera* leaves extract @ 500 mg/kg body weight showed superior efficacy by restoring liver biochemical parameters near control levels and markedly improving tissue histoarchitecture.

Conclusion: This study suggests that nanoformulations significantly enhance the therapeutic efficacy and bioavailability of *M.oleifera*, with confirmation of hepato-protective and nephro-protective potential, highlighting their promise for future drug development strategies targeting liver and kidney diseases.

Keywords: *Moringa oleifera***;** Drug Delivery**;** Silver Nanoparticles**;** Antioxidant**;** Phytomedicine

Introduction:

Since the primordium, human beings and other animal species have been exposed to several chemicals, including environmental toxins and clinically useful drugs. However, with the advancement of medicine and the onset of the industrial revolution, exposure to chemicals has also increased. Although some chemicals are beneficial, many have detrimental effects on the environment and pose significant risks to human health. These chemicals can induce cellular damage by generating highly reactive species such as free radicals, which may adversely affect several essential organs of the body, including the liver, kidney, brain, and reproductive system (Unsal et al., 2021, Magalhães and Caldas, 2019).

Liver and kidney are essential organs that maintain the body's homeostasis and ensure efficient metabolism and clearance of exogenous and endogenous substances, including drugs and other environmental toxins. The liver, as the largest exocrine gland, plays a central role in drug detoxification, metabolism, and synthesis of key biomolecules. It also houses several antioxidant enzymes, such as, catalase, glutathione-s-transferase, and superoxide dismutase, as a defense mechanism to counteract the oxidative stress products by chemicals or other exogenous substances (Ullah et al., 2020, Stanley, 2024). The kidney, similarly, plays a crucial role in the metabolism and excretion of drugs and toxic chemical. The renal system is involved in enzymatic transformation of drugs through phase-I and phase-II metabolic reactions, facilitating their excretion through urine, preventing systemic accumulation(Stanley, 2024, Lakshmanan, 2019).

Carbon tetrachloride (CCl_4), is a volatile and colorless organic alkyl halogen, which can be synthesized through chlorination of methane under light (Imtara et al., 2021). Exposure to toxic doses of CCl_4 results in oxidative stress, which is an imbalance between ROS production and the antioxidant defense mechanism of the body. These free radicals can cause damage to vital organs, including the kidney, brain, testis, and other body tissues, with the liver being particularly susceptible. These toxic properties of CCl_4 make it an ideal compound for experimentally induced liver and kidney toxicity (Zargar and Wani, 2021).

Damage to the liver and kidney can be indicated by several biochemical markers and histological alterations, including the concentration of organ-specific enzymes and microscopic changes in tissue architecture. Studies have shown that liver damage can cause a significant increase in liver-associated enzymes, such as alanine aminotransferase (ALT), aspartate aminotransferase (AST), and a decrease in total bilirubin and protein concentration. Renal injury is often marked by an increase in serum creatinine, uric acid, and Blood urea nitrogen (BUN) (Khan and Zehra, 2013, Shehzadi et al., 2019).

Traditional medicine and its therapy have a major impact due to the inclusion of certain medicinal plants all over the world. According to the World Health Organization (WHO) the usage of herbal products accounts for 65-80% of the world's population(Shaban et al., 2016).Having a complex mixture of bioactive compounds, phytogenic products have shown remarkable properties, such as antimicrobial, antiviral, antioxidant, and also sedative properties(Irum Shehzadi et al., 2020). Although plant-based medicines have excellent effects on the individual's

health, most of these medicines have poor bioavailability. According to Biopharmaceutical Classification System (BCS), phytogenic medicines have low solubility and permeation; making their bioavailability comparatively lower compared to other classes of drugs. To overcome this problem, several kinds of bio-enhancers are being studied (Patel et al., 2022).

Moringa oleifera, which belongs to the family moringaceae, contains phytochemicals that protect the liver and kidney from oxidative stress induced by chemicals or heavy metals. Seeds, leaves, roots, and other parts of these plants contain several important nutrients and antioxidant components, including Vitamin-C, flavonoids, β-carotene(Abdel Fattah et al., 2020). However, one of the key challenges during the treatment of oxidative stress is delivering the therapeutic ingredients to the target site. Many studies have proved that antioxidant ingredients found in *Moringa oleifera* have poor absorption(Swetha et al., 2018).

To overcome the challenges associated with the poor solubility, stability and limited bioavailability of plant-based therapeutics, nanotechnology has emerged as a powerful tool for enhancing targeted drug delivery. Among various approaches, metallic nanoparticles- particularly those synthesized from Silver, Zinc, Copper and gold—have demonstrated significant potential in improving the pharmacokinetic profiles of phytomedicine(Mukkavalli et al., 2017, Ghiuță and Cristea, 2020). These nanoscale carriers offer enhanced cellular uptake, controlled release, and site-specific delivery, thereby maximizing therapeutic efficacy while minimizing systemic toxicity. Given these promising developments, the present study aims to evaluate the hepatoprotective and nephro-protective potential of silver nano-based formulation of *Moringa oleifera.* This innovative formulation is intended to overcome the conventional limitation of phytomedicine and provide a more effective therapeutic approach for the treatment of liver and kidney diseases.

2. Materials and Method

2.1 Plant material collection, Identification and Ethical Compliance: Fresh leaves of *Moringa oleifera* were obtained from the Botanical garden from University Research Farm at Koont, PMAS-Arid Agriculture University, Rawalpindi, with prior permission from the authorized departmental authority. A voucher specimen was prepared through pressing, drying and mounting on standard herbarium sheet, identified with the help of flora by Prof. Dr. Rahmatullah Qureshi and deposited as voucher (PMAS-1621) at the PMAS-Herbarium, Pir Mehr Ali Shah Arid Agriculture University, and Rawalpindi.

The species is not listed as endangered or at risk of extinction, and therefore, no conservation- related restrictions were applicable. The collection and use of plant material complied with institutional guidelines and relevant international biodiversity and conservation principles.

2.2 Biosynthesis of *M. oleifera* silver Nanoparticles

2.2.1Preparation of the Leaves Aqueous Extract: Fresh and green leaves of *M. oleifera* were used to prepare the extract. The leaves were thoroughly washed, dried, and non-essential parts of the plants were removed. The clean

leaves were then ground using an electric grinder. The prepared leaf powder was mixed with 100mL of distilled water and heated at 50°C for 2 hours. After filtration, the solution was stored for further processing (Mohammed and Hawar, 2022).

2.2.2 Biosynthesis of AgNPs Using *M. oleifera* Leaves Extract

To prepare a 5 mM solution of silver nitrate ($AgNO_{3)}$, 0.84g of $AgNO_3$ was dissolved in 1000 ml of distilled water. Subsequently, 100ml of the *M. oleifera* leaves extract was added dropwise to the 900ml of the $AgNO_3$ solution under vigorous stirring. The resulting solution was then placed in the microwave at 600 W and the reaction was observed after every 30 seconds until the colour changed from light yellow to dark brown. A visible colour change from light yellow to dark brown indicated the formation of silver nanoparticles (AgNPs). The mixture was centrifuged at 10,000 rpm for 20 minutes. The precipitated AgNPs were then washed twice with ethanol to remove all impurities. The pellets were collected carefully and dried (Mohammed and Hawar, 2022)

2.2.3 Characterization for AgNPs

UV-vis spectophotometry was performed to determine the light absorbance of greenly synthesised silver nanoparticles across the wavelength ranges from 290 to 690nm. Fournier Transform Infrared spectroscopy (FTIR) was performed to check different functional groups associated with capping agents on the nanoparticles. X-ray diffraction was performed to assess the crystallinity and crystal structure of Ag NPs. Size and morphology of the NPs were examined using scanning electron microscopy, while energy dispersive X-ray analysis (EDX) was performed to check the elemental composition of NPs (Asif et al., 2022, Widatalla et al., 2022).

3. Animal and study design

Eighty four male Wister albino rats were purchased from National Institute of Health (NIH), Islamabad and housed at the Department of Veterinary Pathology, PMAS-Arid Agriculture University, in a controlled laboratory environment i.e., at an ambient temperature of 25–30 °C and with a 12-hour each of dark/light cycle. Rats were provided with a *feed pellet* diet and water *ad libitum*. Animal experiment and the experimental protocols were approved by the university ethical committee.

Following acclimatization, rats were divided into 7 groups, with each group consisting of 12 rats. The experimental groups are as follows:

- Group I- Control group;
- Group II-Negative control group with 1ml of CCl4 i olive oil (1:1);
- Group-III 1ml of CCl_4 in olive oil as well as 100mg/kg body weight silymarin as standard drug;
- Group-IV 1ml of CCl4 in olive oil as well as 200mg/kg body weight of *M. oleifera* leaf extract;

- Group-V 1ml of CCl4 in olive oil as well as 500mg/kg body weight of *M. oleifera* leaf extract;
- Group- VI1ml of CCl4 in olive oil as well as 2.5mg/kg body weight of *M. oleifera* leaf extract nanoparticles.

Group-VII1ml of CCl4 in olive oil as well as 4mg/kg body weight of *M. oleifera* Nanoparticles. All the treatments were administered orally for 31 days. At the end of experiment period (day 31), animals were euthanized by cervical dislocation performed by a trained investigator in accordance with in accordance with institution ethical approval and ARRIVE guidelines. No chemical agents were used in euthanasia. Death was confirmed by the absence of respiration, heartbeat, and reflex activity.

Following euthanasia approximately 5 ml of blood was clot activator tubes which were kept in slanting position to facilitate serum separation. Serum was obtained by centrifugation of the blood at for 5 min in 3000 rpm and then processed for analysis of biochemical studies. Liver and Kidney were rinsed in physiological saline and fixed in 10% formalin for histological examination.

3.1 Biochemical Assays: Harvested serum was used for analysis of serum biochemical parameters, alanine aminotransferase (ALT), aspartate transaminase (AST), bilirubin, uric acid, createnine, total protein, total albumin, and total globulin concentration by using auto analyzer (Micro Lab 200, Merck).

3.2 DPPH Scavenging Activity (%): The aqueous extract of *Moringa oleifera* leaves and its greenly synthesized silver nanoparticles were subjected to radical scavenging activity using DPPH (2,2-diphenyl-1-picrylhydrazyl) radical scavenging method described by Ramamurthy, et al.,2022.A 0.1mmol/L methanolic solution was freshly prepared. Various concentrations of *Moringa oleifera* leaves extract and its nanoparticles were prepared (10, 20, 30, 40, and 50 µg/mL) and 5mL of the DPPH solution was added to each sample. The reaction mixtures were vigorously shaken to ensure proper mixing.
Ascorbic acid was used as the standard antioxidant control. The mixtures were then incubated at 27 °C for 20 minutes in the dark to allow the reaction to proceed. After incubation, the absorbance of each sample was measured. The percentage of DPPH radical scavenging activity was calculated using the following mathematical equation:

$$\text{DPPH Scavenging Activity (\%)} = \frac{A_{control} - A_{sample}}{A_{control}} \times 100$$

Where $A_{control}$ is the absorbance of the DPPH solution without sample, A_{sample} is absorbance of the reaction mixture containing the extract and nanoparticles.

3.3. Hydroxyl Radical Scavenging Activity (H_2O_2): H_2O_2 scavenging activity was performed by using the methodology described by Halliwell, 1987. The reaction mixture (1mL total volume) consisted of 100 µL of 2-

deoxy-2-ribose (28mM) prepared in phosphate butter (pH 7.4), 500µL of different concentrations (10-80µg) of *Moringa oleifera* aqueous extract and greenly synthesized nanoparticles, and 200 µL of $FeCl_3$ (200 µM)–EDTA (1.04 mM) solution prepared in a 1:1 (v/v) ratio. Subsequently, 100 µL of hydrogen peroxide (1.0 mM) and 100 µL of ascorbic acid (1.0 mM) were added to initiate the reaction.

The reaction mixture was incubated at 37 C for 60 minutes. Following incubation, the extent of deoxyribose degradation caused by hydroxyl radicals was determined using the thiobarbituric acid (TBA) reaction. The absorbance of the resulting solution was measured t 532 nm using the UV-vis spectrophotometer. The percentage of inhibition of deoxyribose degradation, indicating hydroxyl radical scavenging activity, was calculated using the following formula:

$$\text{DPPH Scavenging Activity (\%)} = \frac{A_{control} - A_{sample}}{A_{control}} \times 100$$

Where $A_{control}$ is the absorbance of the control reaction solution without sample, A_{sample} is absorbance of the reaction mixture containing the extract and nanoparticles.

3.2 Histopathology study: Following decapitation and blood collection, liver and kidney were removed and fixed in 10% neutral buffer formalin for 24 hours. The fixed tissues were properly dehydrated and cleared before being embedded in liquid paraffin wax. Sections of about 5 µm in thickness were prepared and stained with hematoxylin and eosin (H&E) for histopathological examinations. Histopathology will be done by the method described by the (Bancroft and Gamble, 2008).

4. Statistical Analysis: The data collected from treatment trail were presented as a mean ±Standard deviation. Data was analyzed by one way analysis of variance (ANOVA) by using Minitab Statistical Software (Version 22.2.2). A $p<0.05$ was appointed as the level of significance.

5. Results and Discussion

5.1 CHARACTERIZATION OF NANOPARTICLES

5.1.1 UV-Vis spectroscopy

Formation of AgNPs was confirmed by the change in color from light yellow to dark brown due to MO-AgNPs surface plasmon resonance (SPR) (Fig. 5.1). Formation of Nanoparticles was further confirmed by UV-visible spectroscopy, using T60 Visible Spectrophotometer (PG instruments, UK). The wavelength scale was fixed between 290 and 700nm. Maximum absorbance was observed at 454nm (Fig 5.2).

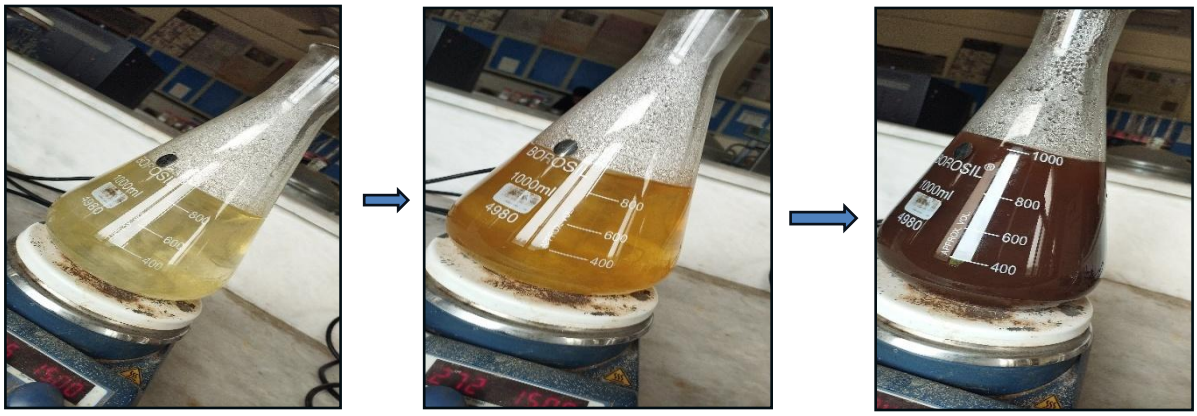

Figure 5.1 (a) Change in Color indicating the synthesis of Nanoparticles

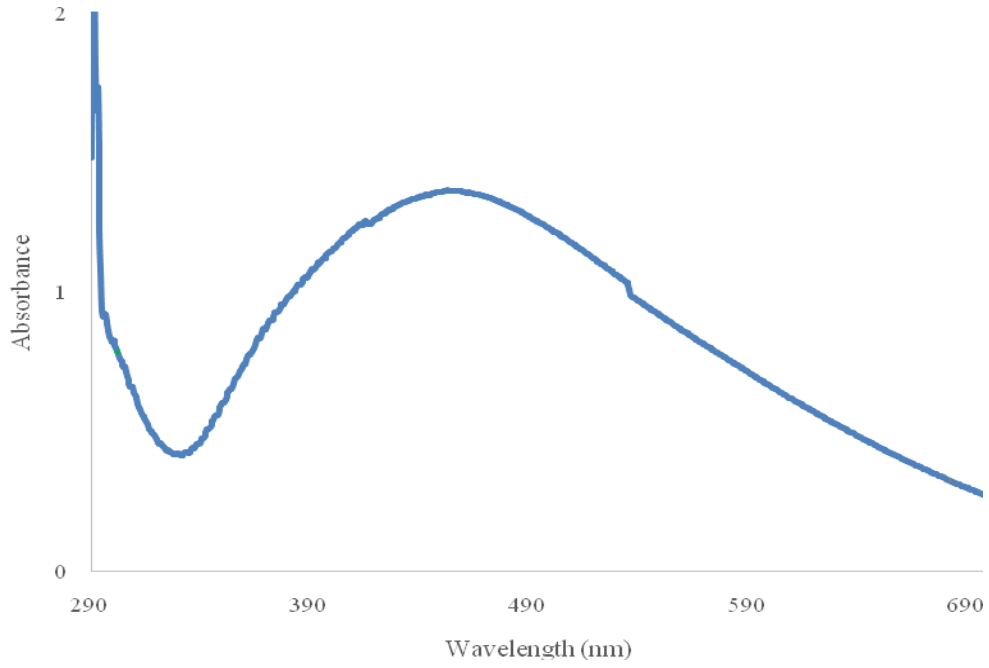

Figure 5.1 (b) UV-Vis spectophotometry indicating peak at 454nm

5.1.2 Fourier transform infrared (FTIR)

FTIR analysis of MO-AgNPs was carried out to check the presence of different functional groups present in synthesized nanoparticles. These functional groups indicate the presence of different biomolecules capped by Silver. A narrow peak at 3419 cm^{-1} indicates the presence of OH group, which may be phenol. Peak at 2918cm^{-1} and 2852cm^{-1} indicates presence of alkenes and Alkynes. Similarly, peak at 2126cm^{-1} indicates carbon-carbon triple bond stretch. Peak at 1630cm^{-1}, 1520cm^{-1} , and 1379cm^{-1} indicate carboxylic, amide and alkene (-C=C-) functional groups, respectively.

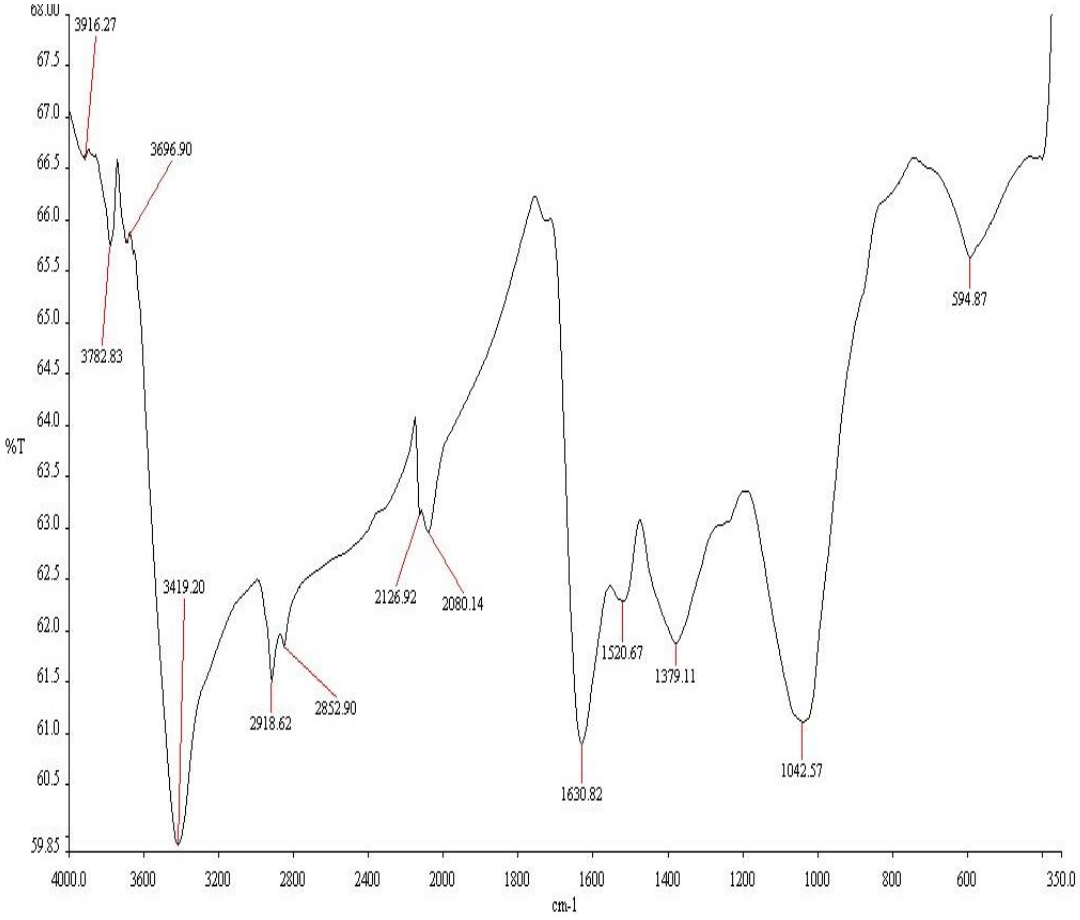

Figure 5.2 FTIR analyses of *M. oleifera* Nanoparticles indicating the characteristic absorption bands corresponding to different functional groups

5.1.3 Scanning Electron Microscopy and EDS

Scanning Electron Microscopy (SEM) was used to examine the morphology and size of the Nanoparticles. Prepared nanoparticles were spherical in shape with an average diameter of 43nm (Fig. 5.4)

To check the elemental composition of AgNPs, Energy-Dispersive X-ray (EDX) was performed indicating the presence of Potassium (K), Oxygen (O), Sulphur (S), and Silver (Ag). Below figures show the size and EDX of the synthesized nanoparticles (Fig. 5.5)

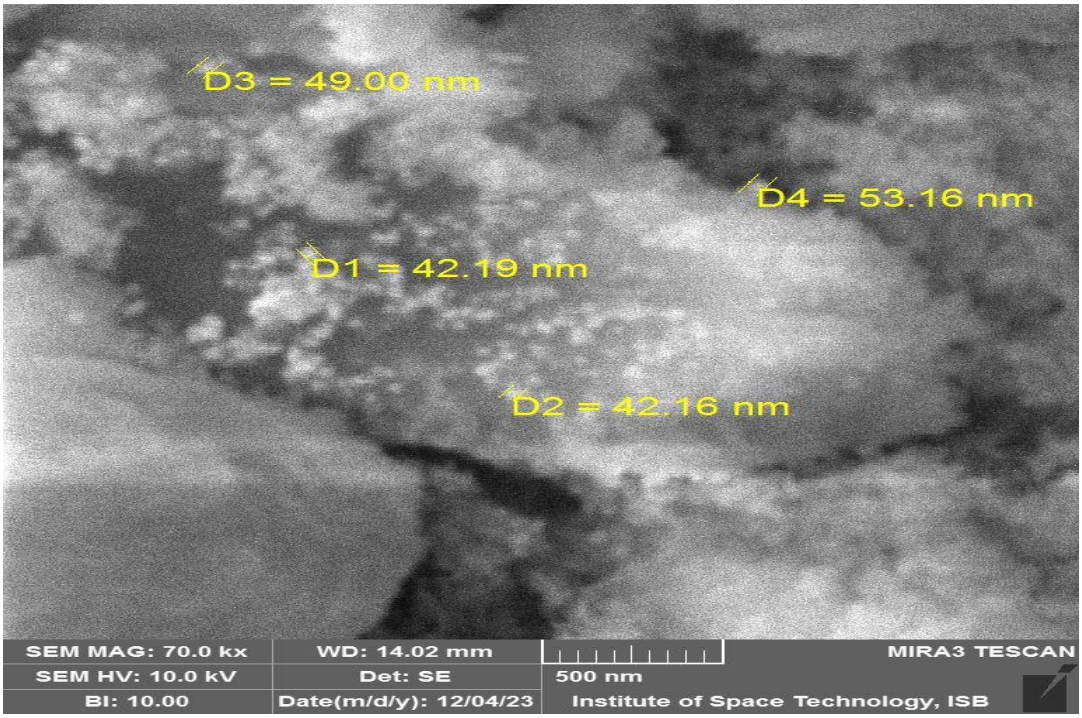

Figure 5.3 (a) Scanning Electron Microscope images showing surface morphology and structural characteristics of MO-NPs.

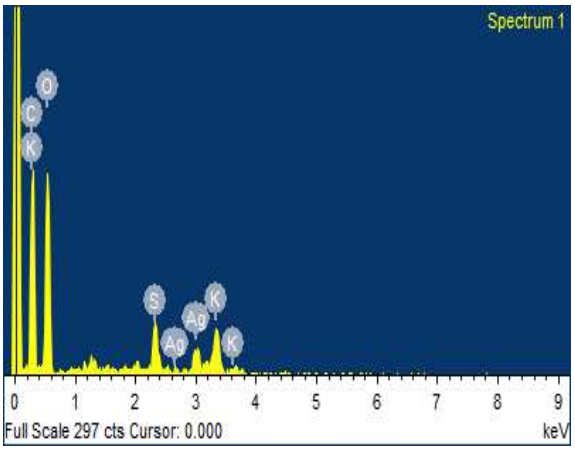

Element	Weight%	Atomic%
C K	37.37	52.92
O K	35.60	37.85
S K	5.84	3.10
K K	10.04	4.37
Ag L	11.15	1.76
Totals	100.00	

Figure 5.3 (b) Energy dispersive X-ray Spectroscopy spectrum showing the elemental composition of the analyzed sample, confirming the presence of major constituent elements.

5.1.4 X-ray diffraction (XRD)

The crystalline nature of the nanoparticles was studied using X-ray diffraction (XRD). The sharp and narrow peaks at different values of 2θ were clear indicative of crystalline nature of nanoparticles. Below image shows the XRD peaks.

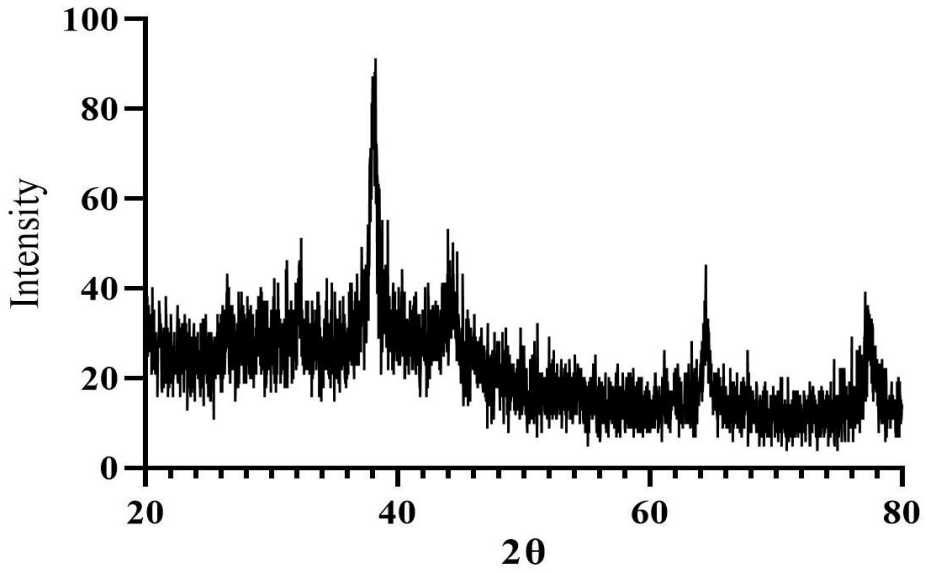

Figure 5.4 X-ray diffraction (XRD) pattern of the analyzed sample indicating characteristic differential peaks corresponding to crystalline phases present the material

5.2 Liver Function Tests

5.2.1 Liver Enzymes

5.2.1.1 Serum ALT:

Serum ALT activity, a sensitive marker of Hepatocellular damage, was significantly elevated in CCl_4 intoxicated group compared to control group *($p < 0.05$),* indicating the successful induction of hepatocellular injury (Table 5.2.1). Treatment with Silymarin showed significantly reduced ALT level compared to CCl_4 group (77.17 ± 1.558 U/L), although the value remained above the control group. Similarly, administration of *Moringa oleifera* demonstrated hepatoprotective effects. MO-1 lowered ALT level to 74.67± 0.882 U/L, a reduction, compared to silymarin, whereas MO-2 showed a more pronounced reduction (52.50 ± 0.719 U/L), appearing near to control group. Notably, nanoparticles formulation of *M. oleifera* further enhanced the hepatoprotective effects. MO-NPs-1 showed significant decrease in ALT activity (64.67 ± 1.256 U/L), where at MO-NPs-2 exhibited the greater efficacy (52.50 ± 0.719), restoring the serum ALT to values statistically indistinguishable from MO-2 and much closer to control group.

5.2.1.2 Serum AST:

Serum AST activity showed a significant increase in the CCl_4 group compared to control group *(P<0.001),* confirming the induction of hepatocellular injury. Silymarin treated group reduced AST levels to 217.83 ± 0.833 U/L, while MO-1 (206.50 ± 1.544) and MO-NPs 1 (202.33 ± 2.753 U/L) exhibited comparable protective effects. MO-2 further decreased AST activity (182.00 ± 1.000 U/L), and most notable reduction was observed with MP-NP 2 (181.83 ± 1.815 U/L), bringing values closer to the control group.

5.2.1.3 Serum Bilirubin:

The hepatoprotective effects of crude MO- leaf extract and Ag-NPs was also evaluated by assessing the serum bilirubin level. Rats administered CCl_4 showed a significant increase in bilirubin compared with the control group (*p<0.001*). Treatment with silymarin (1.17 ± 0.057 mg/dL) and MO-1 (1.08 ± 0.053 mg/dL) produced a marked reduction, though values remained higher than normal. MO-2 (0.96 ± 0.021mg/dL) showed stronger effects, while silver nanoparticle formations exhibited the more pronounced activity. MO-NPs 1 (0.92 ± 0.021 mg/dL) significantly decreased bilirubin and MO-NPs 2 (0.088 ± 0.025 mg/dL) restored level near to the control group. These results demonstrate that the both crude MO leaf extract and nanoparticle formations are most effecting in reversing the CCl_4 induced hyperbilirubinemia.

These findings indicate that MO extract, ZnO-NPs, and particularly greenly synthesized Ag-NPs effectively ameliorate CCl_4-induced alterations in liver enzymes with MO-NPs2 showing the greatest restorative effects (Figure 5.2.1 a,b, c)).

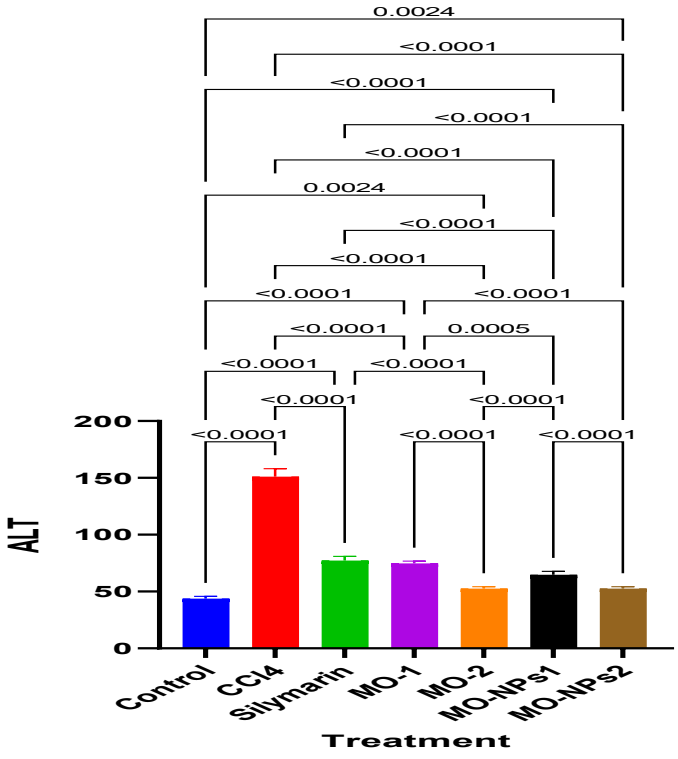

Fig 5.2.1 (a) Comparative distribution of measured variables across study groups, showing variation in response magnitude among different groups, with the CCl_4 group demonstrating the highest observed value and the

MO-AgNPs-2 the lowest (near to control group) under the experimental conditions.

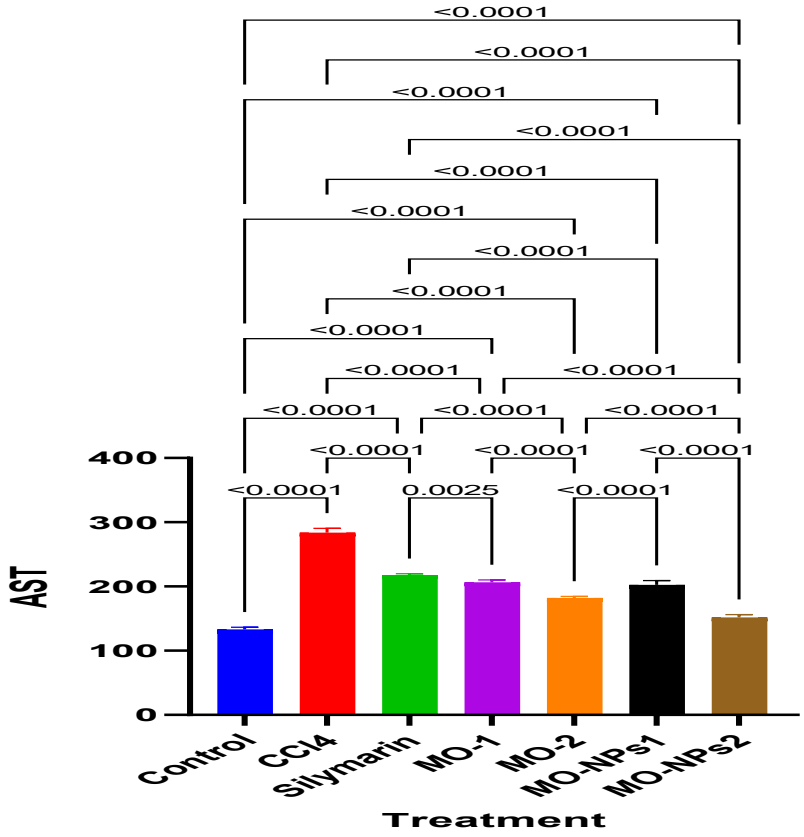

Fig.5.2.1 (a) Comparative distribution of measured variables across experimental groups, demonstrating marked intergroup variation. The CCl_4-treated group exhibited the highest response magnitude, while the MO-AgNPs-2 group showed the lowest values, closely approaching the control group under the experimental conditions.

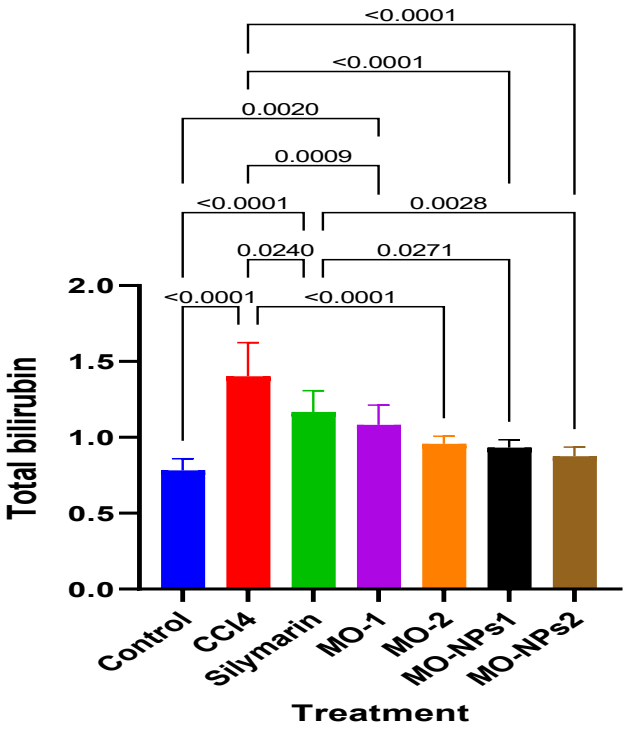

Fig 5.2.1 (c) Comparative distribution of measured variables across experimental groups, demonstrating marked intergroup variation. The CCl_4-treated group exhibited the highest bilirubin concentration, while the MO-AgNPs-2 group showed the lowest values, closely approaching the control group under the experimental conditions.

5.2.2 Total Protein and Albumin Concentration

Serum total protein were markedly reduced in the CCl_4 intoxicate group (4.93 ± 0.071 g/dL) compared to control group (7.90 ± 0.093 g/dL), confirming severe hepatic dysfunction and impaired protein synthesis. Silymarin treatment did not produce any significant recovery (4.90 ± 0.045 g/dL). Administration of crude M. oleifera extract exhibited dose dependent protective effects, with MO-1 showing partial improvement (5.33 ± 0.049 g/dL) and MO-2 producing more pronounced restoration (6.62 ± 0.054 g/dL). Similarly, MO-AgNPs showed a significant improvement with MO-AgNPs showed better recovery (6.32 ± 0.079 g/dL) and AgNPs-2 (7.37 ± 0.095 g/dL) nearly restoring values closer to the control group. Fig (5.2.2 a and b) showed that *Moringa oleifera,* particularly its nanoformulations, improved restoration of hepatic protein synthesis.

A significant decline in serum albumin concentration was observed in the CCl_4 intoxicated group (2.37 ± 0.033 g/dL) compared to control group (3.35 ± 0.052 g/dL), reflecting impaired hepatic synthetic function and compromised protein metabolism. Silymarin administration resulted in only marginal improvement (2.58 ± 0.031 g/dL) indicating limited capacity to restore albumin biosynthesis. Treatment with MO crude extract showed dose dependent effects, with MO-1 partially elevating albumin levels (2.92 ± 0.048 g/dL), while MO-2 further improved synthesis (3.08 ± 0.054 g/dL). Similarly, green-synthesized MO-AgNPs demonstrated a restorative impact, as MO-NPs 1increased albumin to 2.93 ± 0.032 g/dL whereas MO-NPs 2 (3.19 ± 0.051 g/dL) achieved values statistically

compared to the control group. These findings strongly suggest that MO, particularly in its nanoparticle formulation, exerts a potent hepatoprotective effect by ameliorating CCl_4-induced hypoalbuminemia, likely through preservation of hepatocellular integrity and enhancement of protein synthetic machinery.

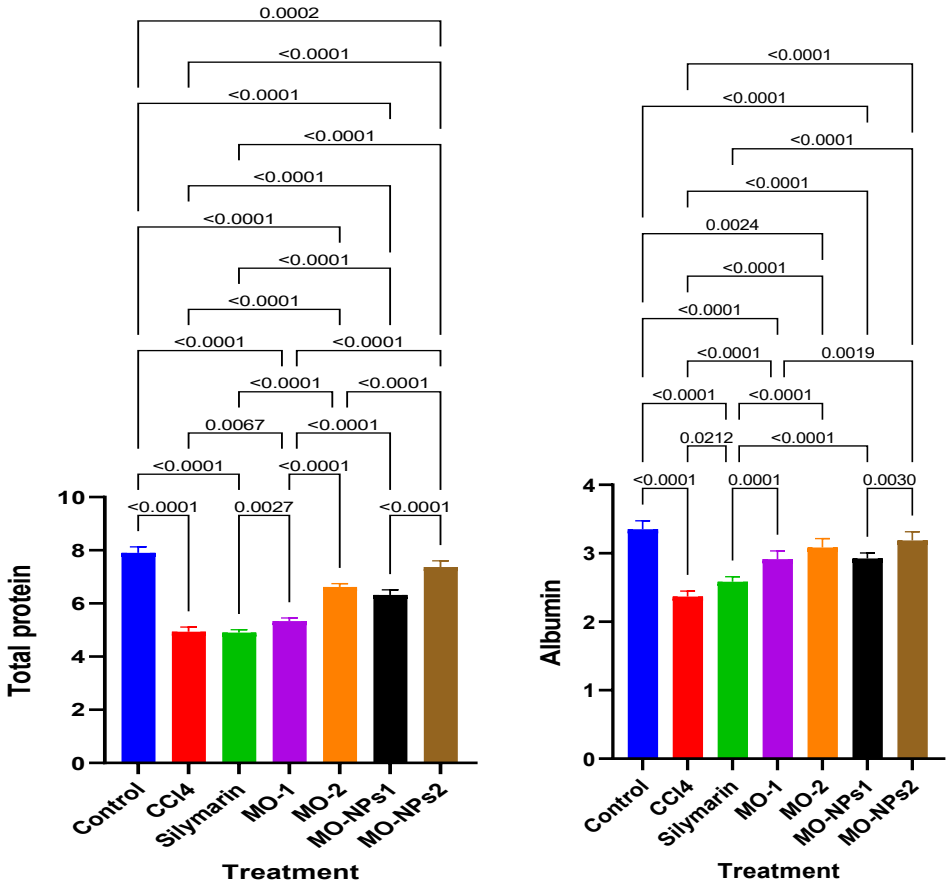

Figure 5.2.2 (a, b): Effect of *Moringa oleifera* (MO), its green-synthesized nanoparticles (MO-AgNPs), and silymarin on serum total protein and albumin levels in CCl_4-induced hepatotoxicity.

Treatment	ALT	AST	Total bilirubin	Total protein	Albumin
Control	43.67±0.88	133.17±1.40	0.78±0.031	7.90±0.093	3.35±0.052
CCl4	151.00±2.88*	283.67±2.79*	1.40±0.090*	4.93±0.071*	2.37±0.033*
Silymarin	77.17±1.56**	217.83±0.83**	1.17±0.057**	4.90±0.045	2.58±0.031**
MO-1	74.67±0.88**	206.50±1.54**	1.08±0.053**	5.33±0.049**	2.92±0.048**
MO-2	52.50±0.72**	182.00±1.00**	0.96±0.0213**	6.62±0.054**	3.08±0.054**
MO-NPs1	64.67±1.26**	202.33±2.75**	0.93±0.0215**	6.32±0.079**	2.93±0.032**
MO-NPs2	52.50±0.72**	151.83±1.82**	0.88±0.0252**	7.37±0.095**	3.19±0.051**

Table 5.1 Effects of *Moringa oleifera* mediated silver nanoparticles on serum biochemical indicators of liver function.

5.3 Renal Function Tests

5.3.1 Blood urea level: Carbon Tetrachloride (CCl_4) administration markedly altered renal function biomarkers compared to control group. A significant elevation in blood urea level was observed in the CCl_4-treated group (45.17 ± 1.249 mg/dL), indicating impaired renal clearance capacity. Conversely, the control group maintained normal urea level (23.83 ± 0.601 mg/dL). Among the treated group, silymarin showed a partial reduction (41.33 ± 0.494 mg/dL), while both *Moringa oleifera* crude extracts (MO-1 and MO-2) demonstrated a more pronounced decline, with MO-2 (33.17 ± 0.946 mg/dL) showing superior efficacy over MO-1 (37.83 ± 0.477 mg/dL). Remarkably, treatment with MO-loaded silver nanoparticles resulted in more substantial amelioration, with MO-NPs 1 (31.50 ± 0.563 mg/dL) and MO-NPs 2 (30.17 ± 0.477 mg/dL) nearly restoring urea level towards normal values, underscoring the enhanced bioactivity of the nanoparticles formulation.

5.3.2 Serum Createnine Concentration: Similarly, serum createnine, another critical indicator of glomerular filtration rate, showed a sharp elevation following CCl_4 administration (1.32 ± 0.040). Silymarin treatment showed a decrease in createnine level (1.10 ± 0.052 mg/dL), though still significantly above control. MO extracts showed dose- dependent protection, with MO-1 (0.87 ± 0.021 mg/dL) and MO-2 (0.67 ± 0.033) showing progressive improvement. Nanoparticle treated groups showed a near-complete normalization of createnine, particularly MO-NPs 2 (0.48 ± 0.031 mg/dL), which was statistically comparable to the control group, suggesting superior nephroprotective potential.

5.3.3 Uric acid: For uric acid, CCl_4 administration resulted in a significant rise (5.68 ± 0.059 mg/dL), nearly doubling the control value (2.67 ± 0.049 mg/dL). Silymarin mitigated this elevation to some extend (4.93 ± 0.033 mg/dL), while MO crude extract groups showed marked improvements, with MO-2 (3.52 ± 0.048 mg/dL) showing greater efficacy than MO-1 (4.23 ± 0.031 MG/dL). Notably, MO-NPs 1 (3.22 ± 0.031 mg/dL) and MO-NPs 2 (2.95 ± 0.043 mg/dL) provided the most significant reduction, with MO-NPs 2 closely approximating the control group.

Collectively, these findings suggest that CCl_4 nephrotoxicity is characterized by elevated urea, createnine, and uric acid levels, reflecting renal impairments. While silymarin offers partial protection, both MO-crude extracts, particularly at higher doses- and nanoformulations substantially restored renal biochemical parameters. The enhanced efficacy of MO-NPs suggests nanoparticles medicated delivery improved bioavailability therapeutical activity, supporting their potential as more effective nephroprotective strategy compared to crude extract or standard reference drug.

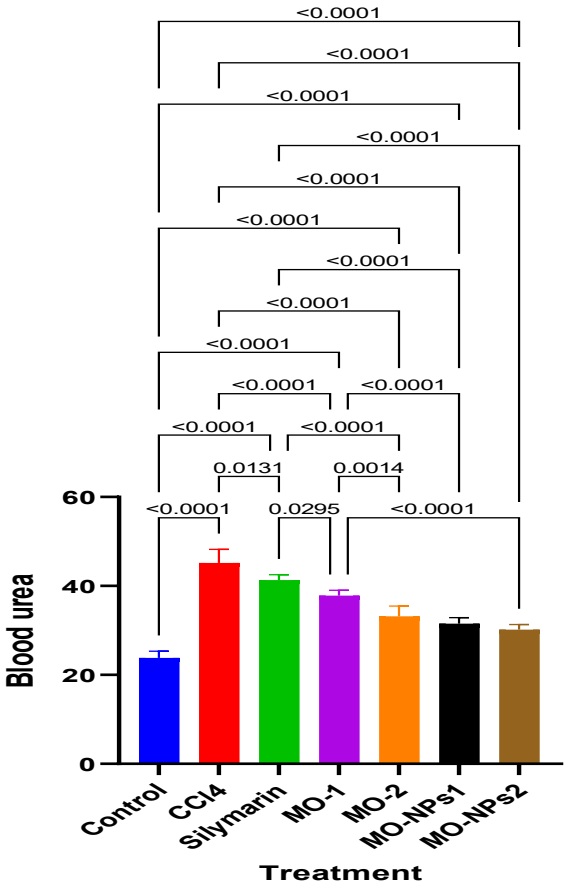

Fig. 5.3.1 (a) Effect of CCl_4 and treatments on blood urea level. CCl_4 caused a significant increase compared to control, while silymarin showed partial reduction. *Moringa oleifera* crude extracts produced dose-dependent improvement, and MO-loaded silver nanoparticles showed the most pronounced restoration, approaching normal values.

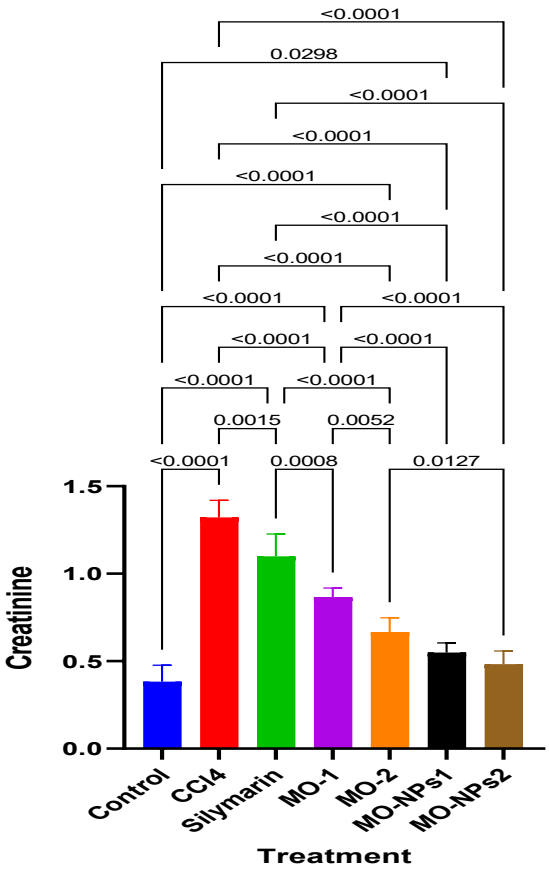

5.3.1 (b) Effect of CCl_4 and treatments on serum creatinine level. CCl_4 significantly elevated creatinine compared to control. Silymarin produced moderate improvement, while *Moringa oleifera* extracts showed dose-dependent reduction. MO nanoparticles exhibited near normalization, with MO-NPs-2 showing the strongest effect.

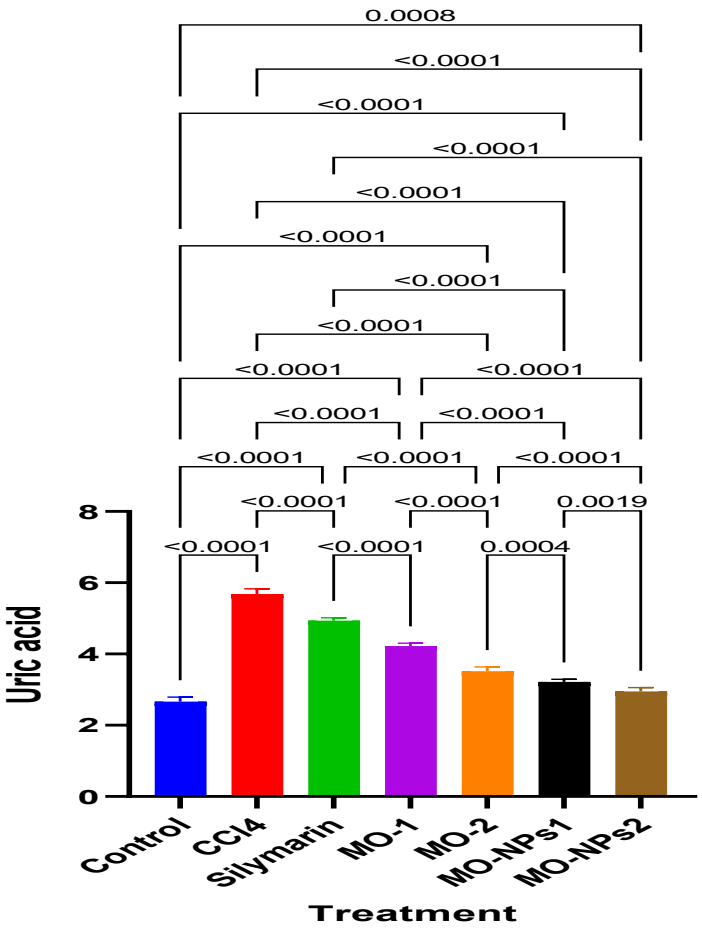

Fig. 5.3.1 (c) Effect of CCl_4 and treatments on serum uric acid level. CCl_4 significantly increased uric acid compared to control. Silymarin caused partial reduction, while *Moringa oleifera* crude extracts showed dose-dependent improvement. MO nanoparticles produced the most marked decrease, approaching control values.

Treatment	Blood urea	Createnine	Uric acid
Control	23.83±0.601	0.38±0.038	2.67±0.049
CCl4	45.17±1.249*	1.32±0.040*	5.68±0.059*
Silymarin	41.33±0.494**	1.10±0.052**	4.93±0.033**
MO-1	37.83±0.477**	0.87±0.021**	4.23±0.031**
MO-2	33.17±0.946**	0.67±0.033**	3.52±0.048**
MO-NPs1	31.50±0.563**	0.55±0.022**	3.22±0.031**
MO-NPs2	30.17±0.477**	0.48±0.0311	2.95±0.043**

Table 5.2 Effects of *Moringa oleifera* mediated silver nanoparticles on serum biochemical indicators of renal function.

5.4 DPPH Scavenging Activity (%): The antioxidant potential of *Moringa oleifera* aqueous extract and synthesized silver nanoparticles was evaluated using scavenging assay. Both the plant extract and nanoparticles exhibited concentration dependent free radical scavenging activity. As the concentration of the sample increased, the percentage of inhibition of DPPH radicals also increased.

The *Moringa oleifera* aqueous extract demonstrated notable antioxidant activity with maximum DPPH radical scavenging activity of approximately 80% at 50µg/mL, whereas synthesized silver nanoparticles showed comparatively higher scavenging activity of around 85 to 88% at same concentration. Ascorbic acid, used as standard antioxidant, show the highest activity with 90% inhibition at 50 µg/mL (Fig. 5.7)

5.5 Hydroxyl Radical Scavenging Activity (H_2O_2): Both the *Moringa oleifera* aqueous leaf extracts and green-synthesized silver nanoparticles exhibited a significant hydroxyl radical scavenging activity in a dose dependent manner. As the concentration of sample increased from 10µg/mL to 50µg/mL, the percentage inhibition of hydroxyl radical also increased. The synthesized AgNPs showed comparatively higher scavenging activity, showing a maximum inhibition of appromixtaely 85 to 90% at 50µg/mL, whereas the *Moringa oleifera* crude extract showed around 80% inhibition at same concentration (Fig 5.8)

Vitamin E, used as the positive control, exhibited the highest scavenging activity, with **more than 90% inhibition** at 80 µg/mL. These findings suggest that the green-synthesized AgNPs possess enhanced hydroxyl radical scavenging potential compared to crude plant extract.

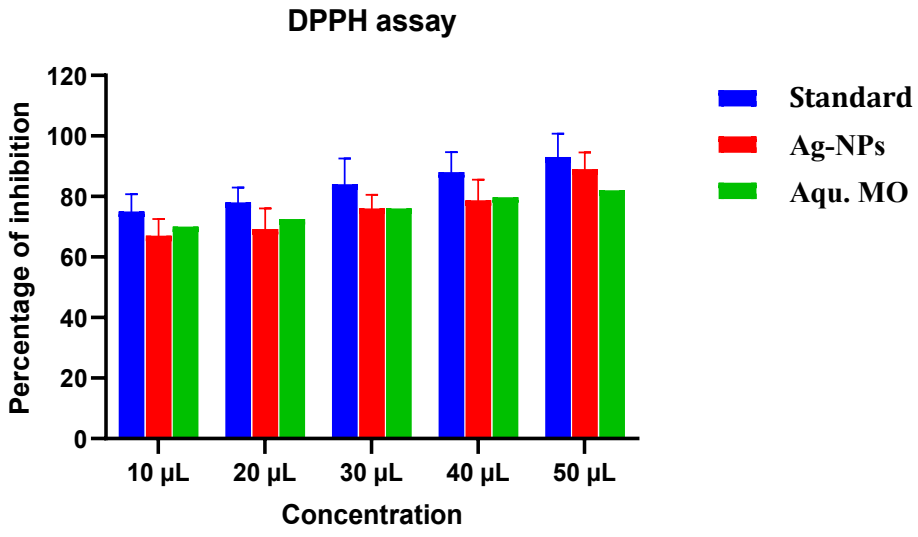

Figure 5.7 DPPH assay indicating high % of inhibition by standard antioxidant followed by Ag-NPs and aqueous extract of *Moringa oleifera*

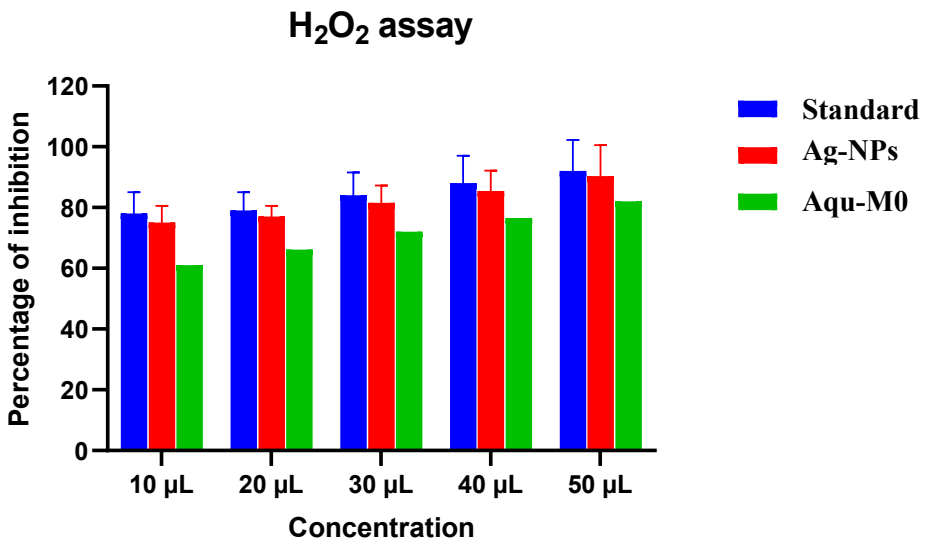

Figure 5.7Hydroxyl radical scavenging assay indicating high % of inhibition by standard antioxidant followed by Ag-NPs and aqueous extract of *Moringa oleifera*

5.4 HISTOPATHOLOGY

5.4.1 Liver

Histopathological studies were performed to examine the damage caused by the oral administration of CCl_4 and recovery through administration of *M.oliefera* crude extract and its AgNPs. Control group showed normal hepatic histoarchitecture. Hepatocytes were arranged in radiating cords extended from central vein towards the portal triads. The Hepatocytes showed uniform polygonal morphology with eosinophilic granular cytoplasm and centrally placed round nuclei. The sinusoids were clearly visible maintaining their normal radial orientation. The portal triads were normal in structure, consisting of portal vein hepatic artery and bile ductile without any evidence of congestion and inflammatory infiltrates. There were no fatty changes, vacuolar degeneration, or fatty change observed (Figure 5.7).

CCl_4 treated group showed profound alteration in hepatic parenchyma, characterized by extensive hepatocellular vacuolation consistent with macro vesicular steatosis, ballooning degeneration, and cytoplasmic rarefraction. Hepatocytes nuclei were frequently placed peripherally. Sinusoidal spaces appeared compressed due to hepatocellular swelling (Figure 5.8).

Silymarin treated group showed mild recovery of Hepatocytes toward normal architecture. There was mild vacuolation, low infiltration at some places, and dilation of sinusoids and no prominent nucleus (severity less than CCl_4 group) (Figure 5.9).

*M. oleifera*crude extract @300 mg/kg demonstrated a marked decrease in inflammation, reduced vacuolation, slight derangement of cytoplasm with no prominent nucleus, and cells infiltration (Figure 5.10).*M. oleifera* crude extract @500 mg/kg showed better recovery with a significant decrease in inflammation, no vacuolation, normal arrangement of Hepatocytes with eosinophilic granular cytoplasm and centrally placed well preserved round nuclei. The sinusoids were slightly deranged but overall architecture was near to normal, indicating the effectiveness of *M.oliefera* against liver diseases (Figure 5.11).

M. oleifera AgNPs @2.5mg/kg revealed a marked a marked decrease in inflammation with normal Hepatocytes, mild degeneration, cell infiltration, normal cytoplasm with prominent centrally placed nucleus, and intact central vein (Figure 5.12). *M. oleifera* AgNPs @4 mg/kg showed intact central vein, no evidence of inflammation, and vacuolation. Hepatocytes were near to normal with cytoplasm and centrally placed round nuclei. The sinusoids were clearly visible with their normal radial orientation. Hepatic architecture was near to normal (Figure 5.13).

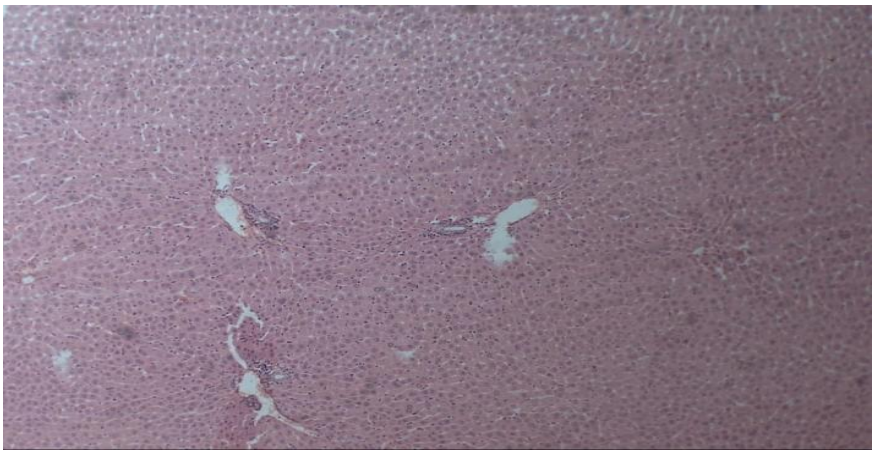

Fig. 5.7 Histopathological section of liver tissues from the control group showing normal architecture.

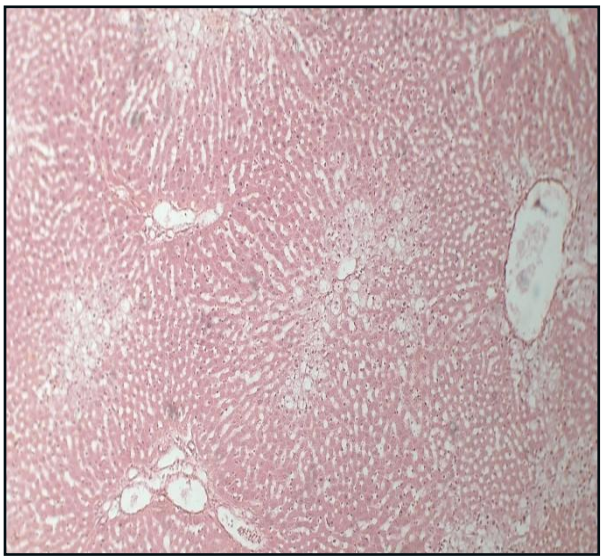

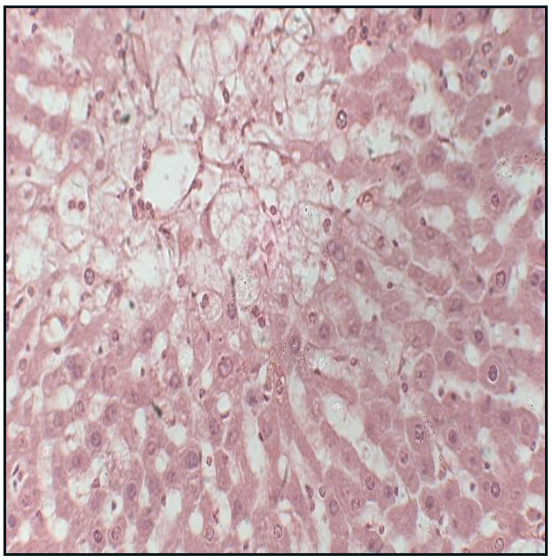

Fig 5.8H&E stained section from the CCl_4 treated group, showing severe hepatic injury characterized by extensive hepatocellular vacuolation, macrovesicular steatosis, ballooning generation, cytoplasmic rarefraction and peripheral displacement of nuclei

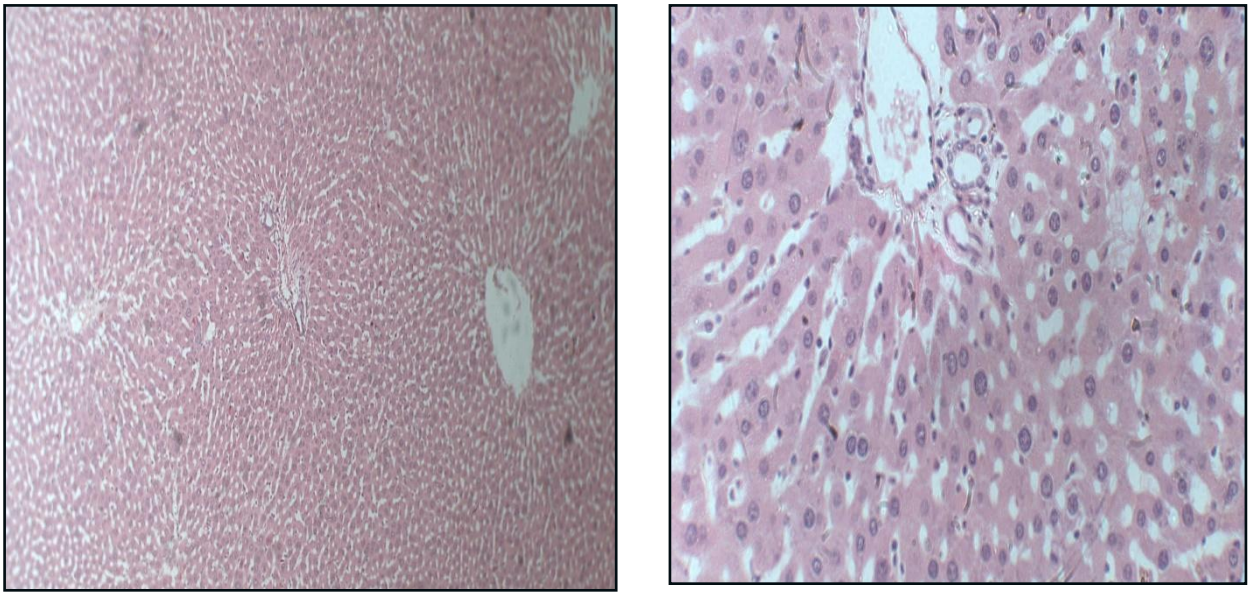

Fig 5.9 Liver section from silymarin treated group indicating partial restoration of hepatic architecture with mild hepatocellular vacuolation, inflammatory cell infiltration, and mild sinusoidal dilation compared to CCl_4 Treated group

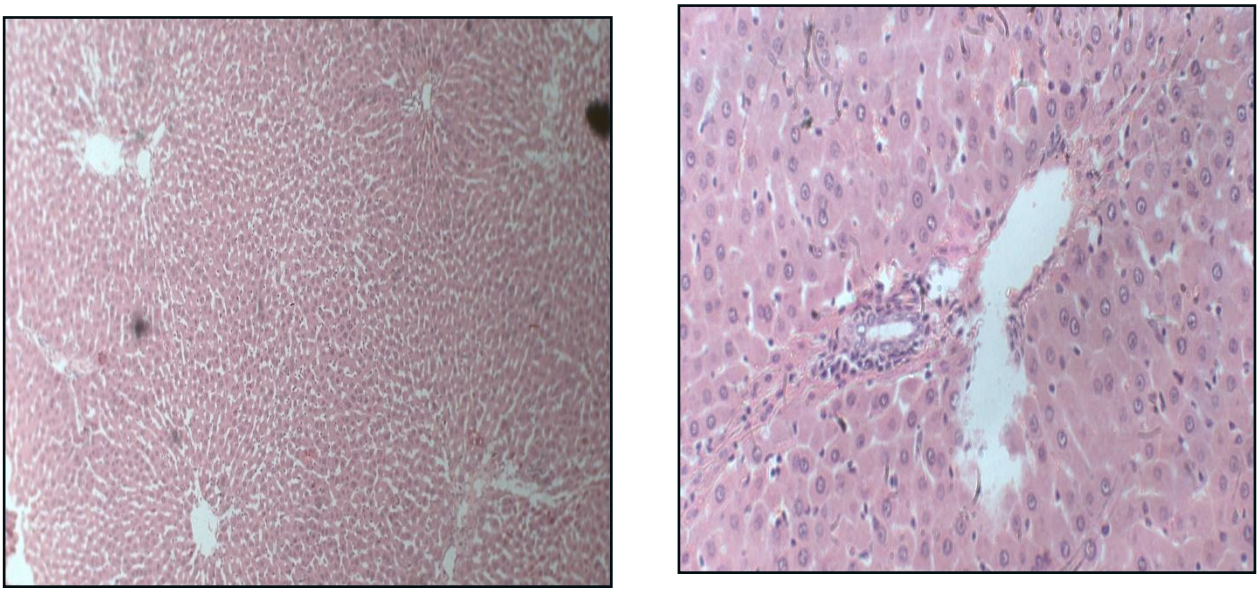

Fig 5.10 Liver sections from rats treated with *Moringa oleifera* crude extract (@300 mg/kg body weight) showing reduced hepatocellular vacuolation, mild inflammatory cell infiltration, and slight cytoplasmic derangement, indicating partial hepatoprotective activity.

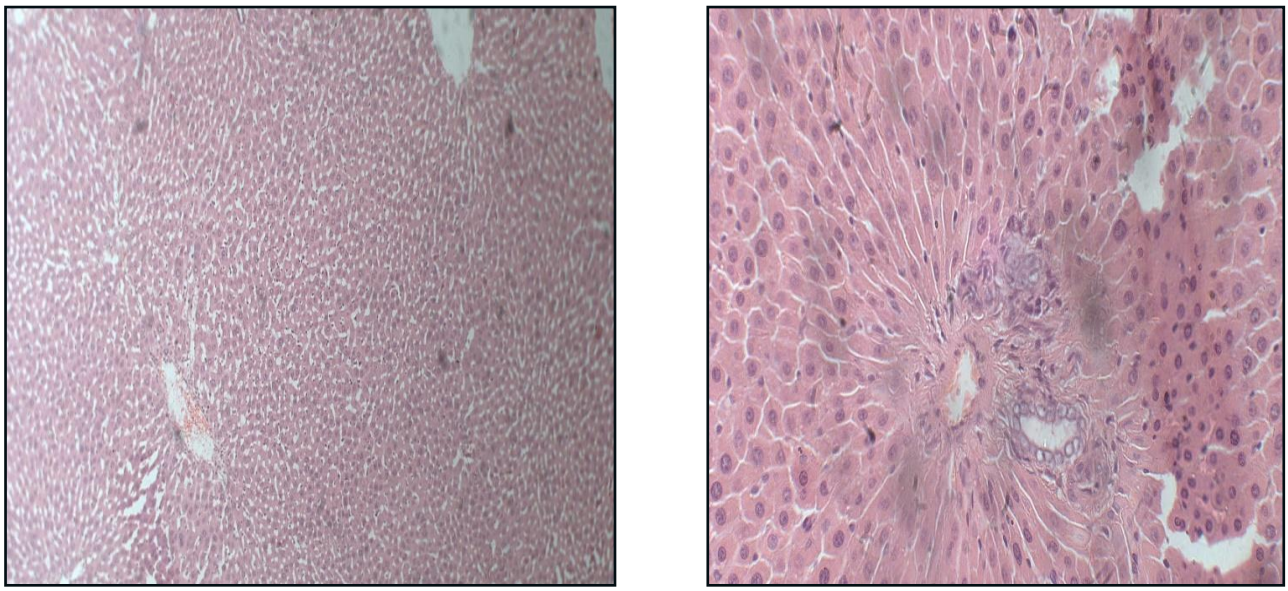

Fig 5.11 H&E staining of liver section from rat treated with *Moringa oleifera* crude extract (@500 mg/kg body weight) indicating marked recovery of hepatic architecture with normal hepatocytes arrangement, eosinophilic cytoplasm, centrally located nuclei, and mild degeneration of sinusoidal spaces.

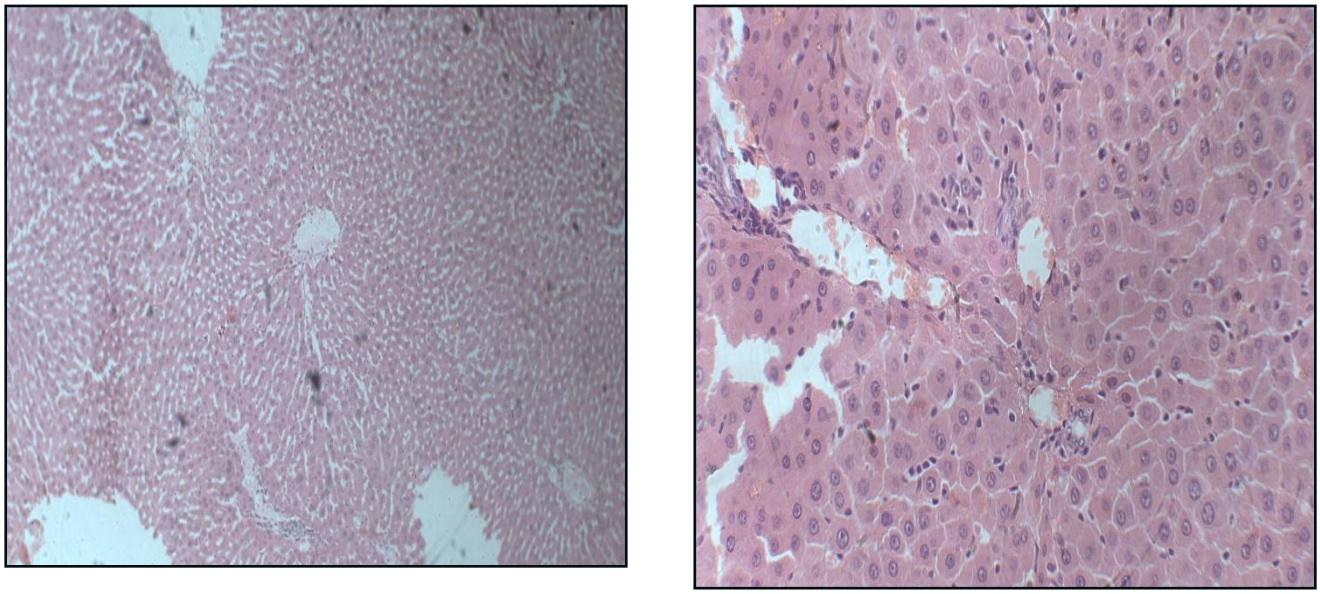

Fig 5.12Liver section from rats treated with *Moringa-oleifera* mediated silver nanoparticles @ 2.5 mg/kg body weight showing reduced inflammatory cells infiltration, normal hepatocytes, intact central vein, and slight congestion

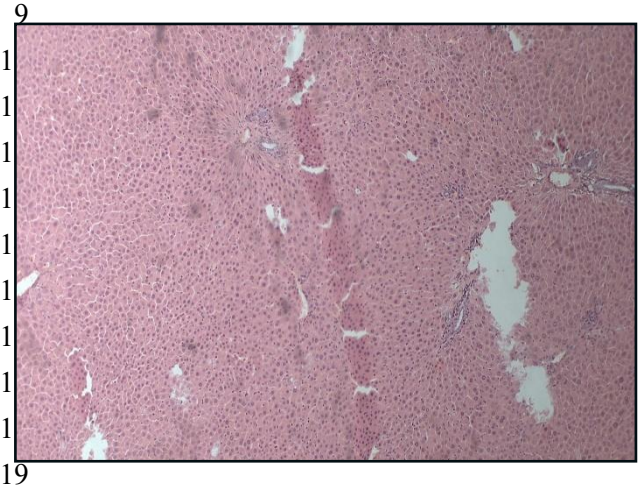

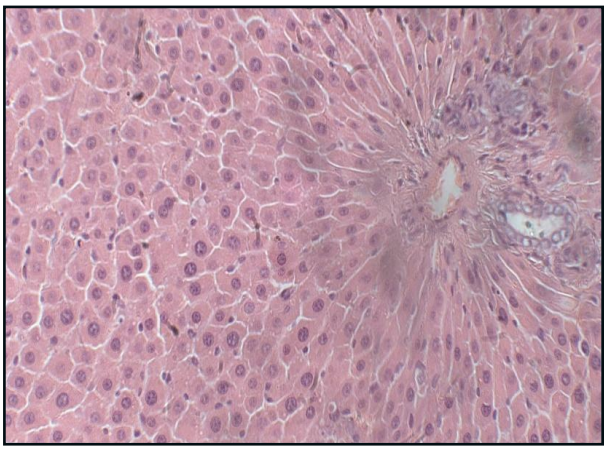

Fig 5.13 Liver sections from rats treated with *Moringa-oleifera* mediated silver nanoparticles @ 4 mg/kg body weight showing near normal hepatic architecture, normal hepatocytes with centrally placed nuclei, well defined sinusoidal spaces, and no inflammatory cell infiltration, indicating complete recovery

5.4.2 Kidney

Control group showed normal histoarchitecture(Fig 5.14). CCl_4 treated group showed severe tubular damage, tubular dilation, glomerular atrophy and devastation of Bowman's capsule. Severe hydropic degeneration of tubular epithelium and tubule epithelium scattered on tubular lumen were also observed in CCl_4 treated group (Fig 5.15).

Silymarin treated group showed a mild recovery in contrast to impairments caused by CCl_4 treatment. However, severe epithelial desquamation, damaged Bowman's capsule, glomerular and tubular degeneration, and congestion were observed in this treatment group(Fig 5.16).

M.oleifera crude extract @ 300 mg/kg showed better recovery compared to positive control group. However, histoarchitecture of this group showed mild congestion, cells infiltration, and damage to Bowman's capsule. Epithelial cell desquamation and damage to tubular degeneration were also observed(Fig 5.17). *M.oliefera* crude extract @ 500 mg/kg showed significant improvement with normal Bowman's capsule, no cell infiltration, mild desquamation, and slight congestion. Renal tubules and Glomerulus was near to control group(Fig 5.18).

Oral administration of *M.oliefera* AgNPs @ 2.5 mg/kg after treatment with CCl_4 showed a slight damage to Bowman's capsule, mild desquamation, moderate congestion, and a slight damage to renal tubules (Fig 5.19). Histoarchitecture of *M.oliefera* AgNPs @ 4 mg/kg was near to control group with no desquamation, a mild congestion, and normal renal tubules and Glomerulus. The Bowman's capsule shape was reversed with normal space, indicating the significant healing in damaged tissue(Fig 5.20).

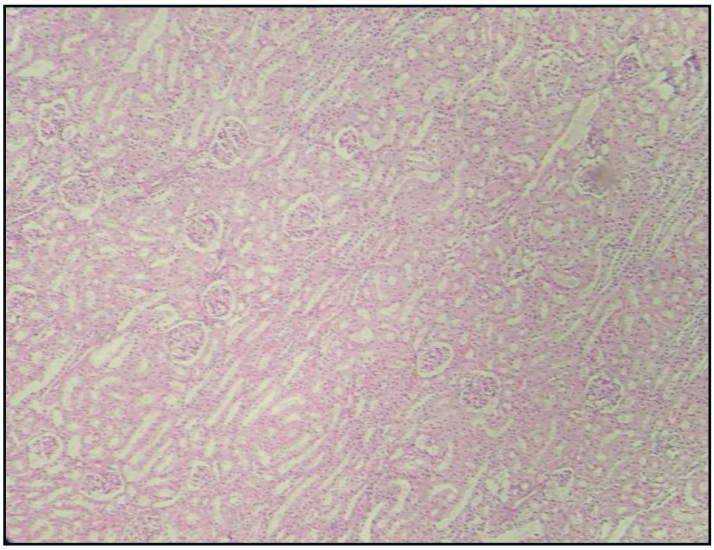

Fig. 5.14 Histopathological section of kidney tissue from control group showing normal renal architecture with intact glomeruli, normal Bowman's capsule, and well organized renal tubules.

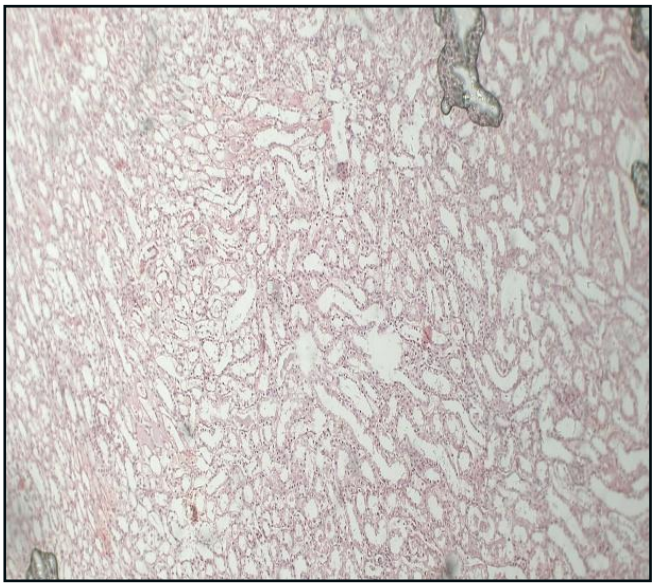

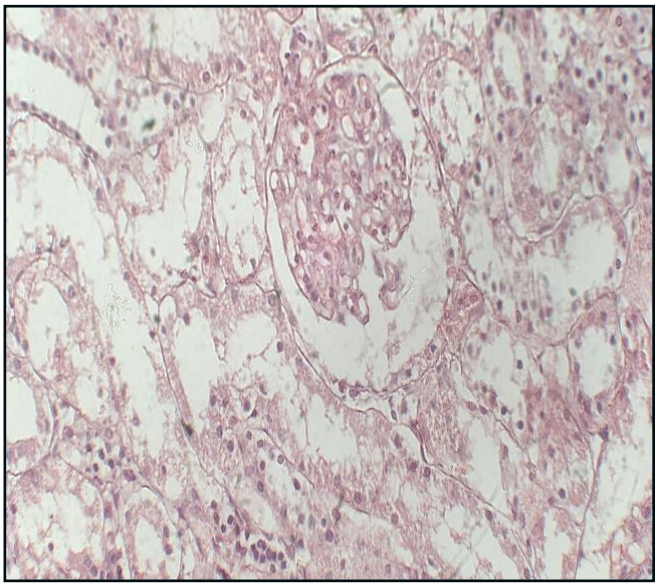

Fig. 5.15 H&E stained section from CCl_4 treated group indicating severe renal damage characterized by tubular dilation, tubular epithelial degeneration, glomerular atrophy, and disruption of Bowman's capsule. Hydropic degeneration of tubular epithelium and epithelial cell desquamation within the tubular lumen are also evident

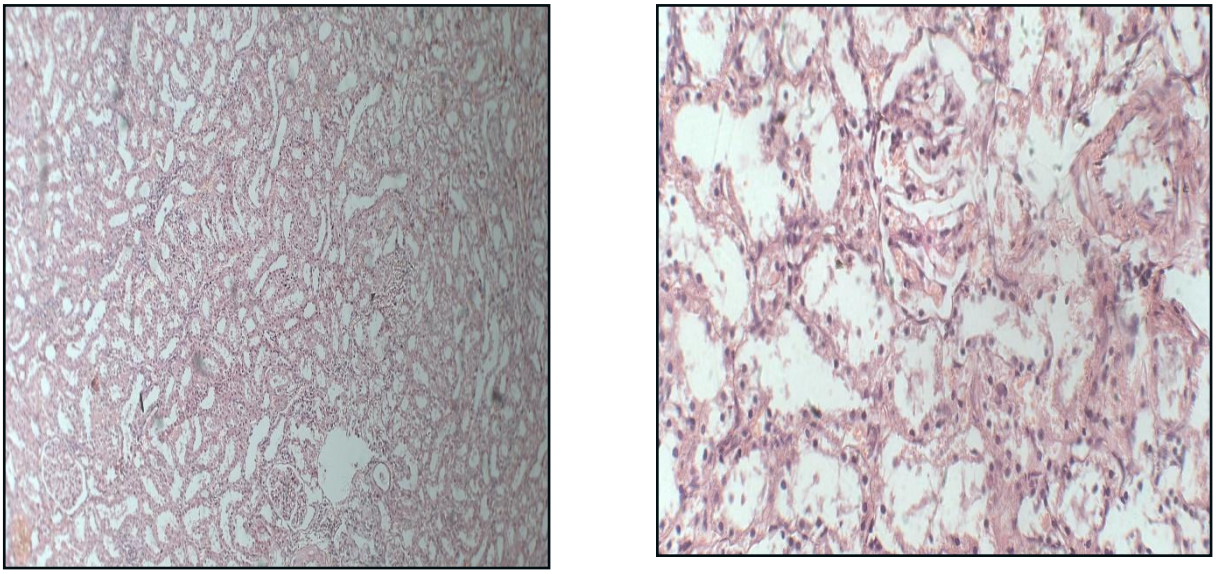

Fig. 5.16 Kidney section from the Silymarin-treated group showing severe epithelial degeneration, damage to Bowman's capsule, tubular damage congestion

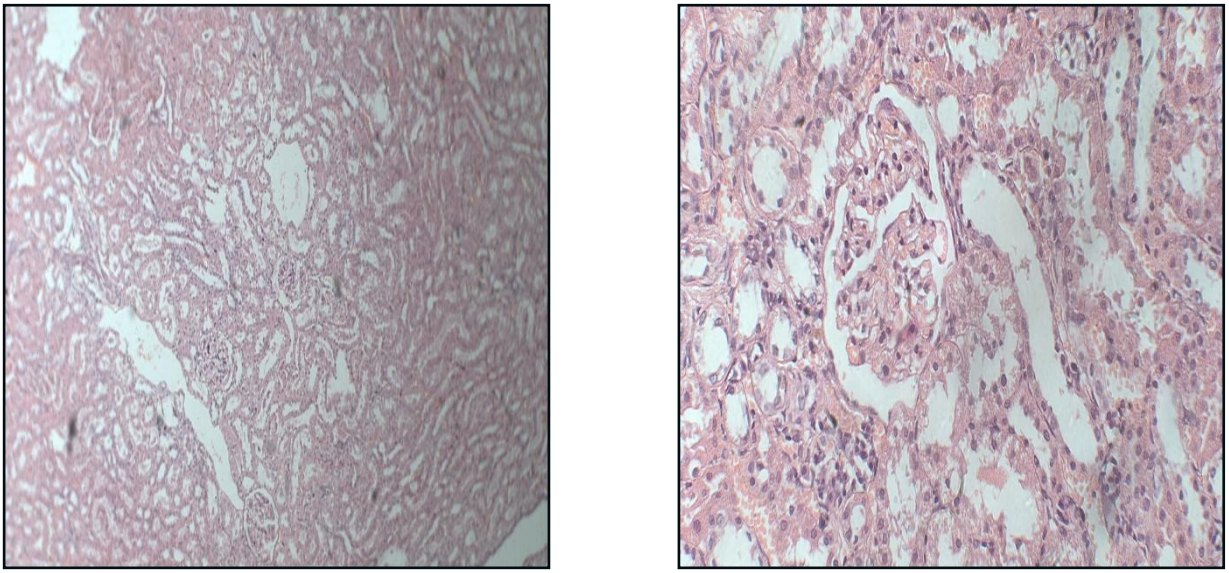

Fig. 5.17 Kidney section from rats treated with *Moringa oleifera* crude extract (@300 mg/kg body weight) showing moderate improvement with reduced tubular degeneration, mild congestion, inflammatory cell infiltration, epithelial desquamation and partial damage to Bowman's capsule

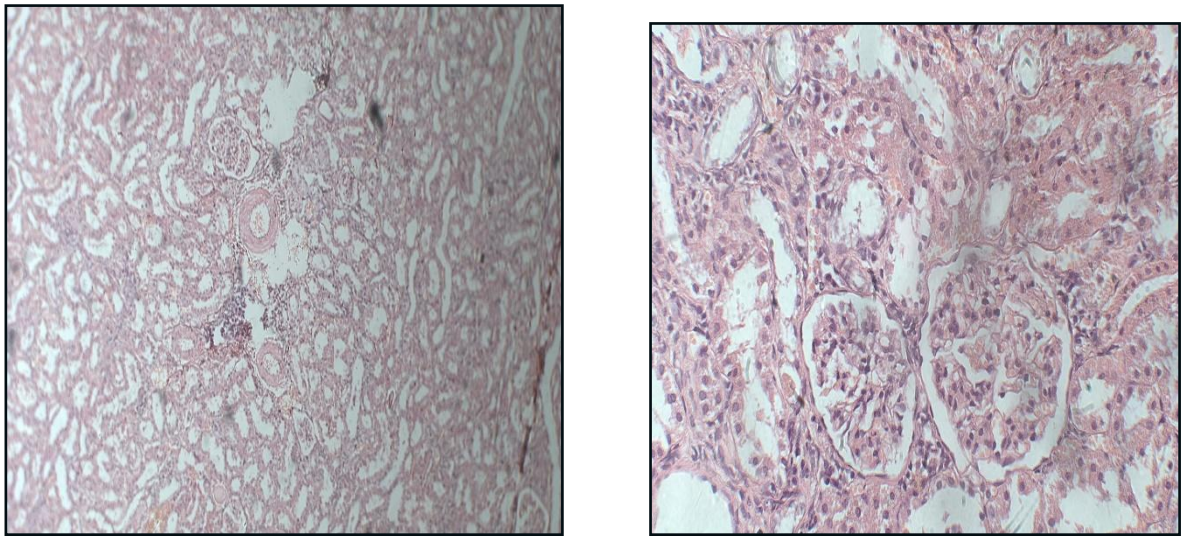

Fig. 5.18 Kidney section from rats treated with *Moringa oleifera* crude extract (@500 mg/kg body weight) indicating significant recovery with near normal renal architecture. Bowman's capsule and glomeruli appear largely normal with slight congestion, and mild epithelial desquamation

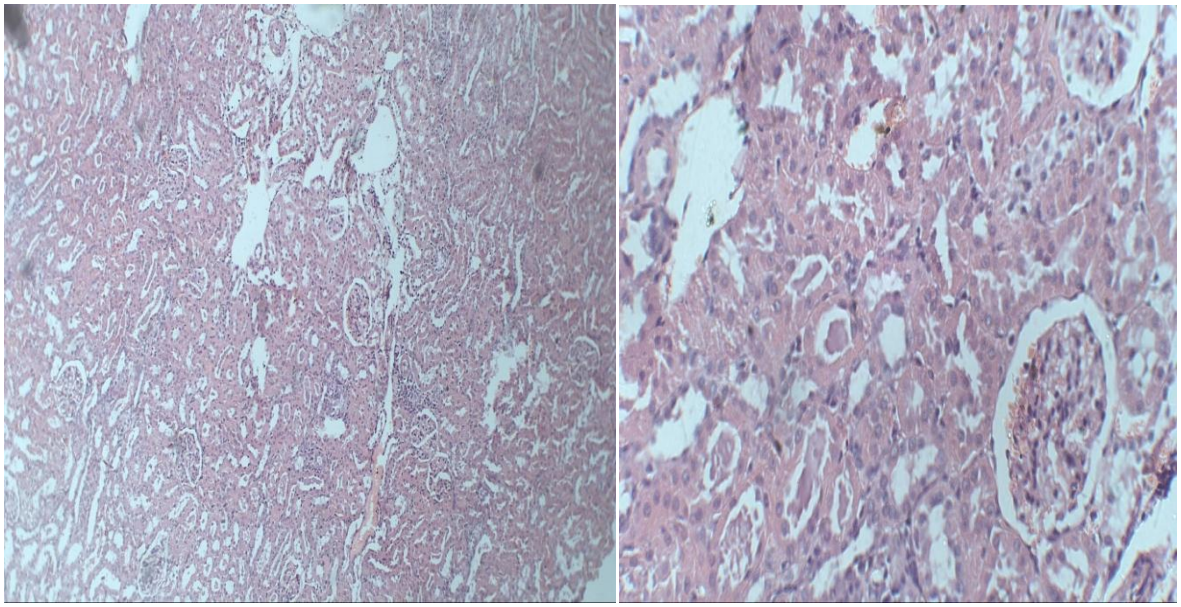

Fig. 5.19Kidney sections from rats treated with *Moringa-oleifera* mediated silver nanoparticles @ 2.5 mg/kg body weight showing mild damage to Bowman's capsule, mild congestion, slight tubular degeneration, and mild epithelial desquamation

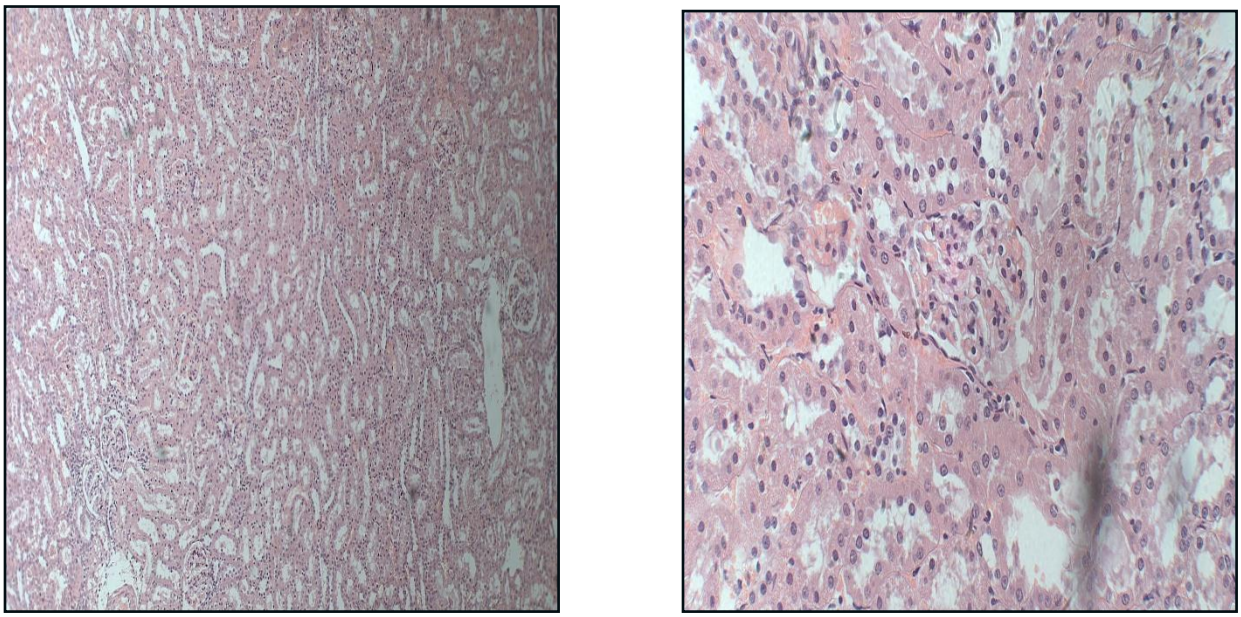

Fig. 5.20 Kidney sections from rats treated with *Moringa-oleifera* mediated silver nanoparticles @ 2.5 mg/kg body weight indicating near-normal renal histoarchitecture, with intact glomeruli, restored Bowman's capsule, and normal renal tubules, with slight congestion, indicating significant recovery from damage

6. Discussion

The liver and kidneys are vital organs responsible for metabolism, detoxification, and excretion of xenobiotic compounds, making them a primary target to heavy metal, environmental pollutants, and drug-induced injury. Exposure to heavy metals, environmental pollutants and several types of medicines-including chemotherapeutic agents-can induce oxidative stress, leading to variety of pathological alteration, including hepatorenal damage (Chang et al., 2023, Lang et al., 2025). Hepatic and Renal diseases are major cause of morbidity and mortality throughout the globe. Worldwide, liver diseases are responsible for nearly 2 million cases of morbidity and mortality, annually. Similarly, approximately 11.5 million cases of renal dysfunction are reported each year in developing countries(Zhang et al., 2023). The increasing prevalence of these conditions underscores the urgent need of accessible and effective therapeutic strategies with least side effects.

Medicinal plants have been used for centuries to prevent and treat liver and kidney diseases. *Moringa oleifera*, commonly known as “Miracle tree” or “Tree of life” is an important member of *Moringaceae* family and contains numerous bioactive compounds such as flavonoids, carotenoids, saponins, tocopherols, and omega fatty acids (Chiș et al., 2023, Pop et al., 2022). These bioactive play a vital role in supporting liver and kidney health (Nurhayati et al., 2024, Attah et al., 2022).

The present study demonstrated the hepatorenal protective effects of *M.oliefera* leaf crude extract and *M.oliefera* based silver nanoparticle (MO-AgNPs) at different doses against experimentally induced liver and kidney damage. This study involved the synthesis of silver nanoparticles and characterization through UV-visible, SEM, FTIR-Analysis, and EDS. In the UV-visible analysis, the AgNPs displayed a prominent peak at 454nm, correspondence to the surface plasmon resonance characteristic of AgNPs. Strong peak at 3keV by the AgNPs, confirmed the presence of Silver, Oxygen, Sulfur, and Potassium. SEM analysis demonstrated that most nanoparticles size ranged between 42nm to 53nm.

FTIR analysis showed multiples peaks at different wavelength, indicating the presence of different functional groups. A narrow peak at 3419 cm^{-1} indicates the presence of OH group, which may be phenol. Peak at 2918cm^{-1} and 2852cm^{-1} indicates presence of alkenes and Alkynes. Similarly, peak at 2126cm^{-1} indicates carbon-carbon triple bond stretch. Peak at 1630cm^{-1}, 1520cm^{-1} , and 1379cm^{-1} indicate carboxylic, amide and alkene (-C=C-) functional groups, respectively.

Administration of CCl_4 in the positive treatment group caused a significant increase in the concentrations of liver and kidney biomarkers, including ALT, AST, bilirubin, serum urea, creatinine, and uric acid. CCl_4 is metabolized by cytochrome P450 to form a trichloromethyl radical (•CCl_3), which is further converted to a trichloromethyl peroxy radical (•$OOCCl_3$), under aerobic conditions. Thee reactive radicals binds to cellular macromolecules and induce lipid peroxidation, leading to membrane damage and leakage of cellular enzymes (He et al., 2022). The oxidative stress induced by CCl_4 disrupts the balance between ROS and antioxidant defenses, causing a significant injury to vital organs, particularly the liver and kidneys, making CCl_4 a widely used compound for experimentally induced acute hepato-renal injury.

Since, *Moringa oleifera* contains several bioactive compounds with antioxidants and anti-inflammatory potential, we hypothesized that our crude extract of *Moringa oleifera* and its greenly synthesized silver nanoparticles (MO-AgNPs) are more likely to alleviate the toxic effects of CCl_4 against hepato-renal injury. To this end, we co-treated animal model with different doses of *Moringa oleifera* (200mg and 500 mg/kg body weight) aqueous extract and their silver nanoparticles (2.5 mg and 4 mg/kg body weight). Since, several adverse effects of silver nanoparticles have also been reported; the doses of the silver nanoparticles used in our study were considerably lower than the concentrations known to cause toxicity.

The enzymes investigated in this study are well-established markers of hepatic and renal functions. Alanine transaminase (ALT) and aspartate transaminase (AST) are primarily located in the cytoplasm of hepatocytes. Under normal physiological conditions, these enzymes remain within the hepatic cells and are not released into the blood stream (Juraev and Shodiyeva, 2026)(Björnsson and Björnsson, 2022). However, hepatocellular damage occurs-often caused by oxidative stress and imbalance between antioxidant and free radical imbalance-results in the leakage of these enzymes into blood, indicating liver injury. Bilirubin is another key indicator of hepatic dysfunction. It is produced due to the breakdown of hemoglobin and is normally processed and excreted by the liver into bile. Impaired liver function results in the accumulation of bilirubin in the bloodstream, results in elevated serum level and clinical signs such as jaundice (Ramírez-Mejía et al., 2024).

Urea and creatinine are well established markers of renal functions and are produced from creatinine phosphate in the muscles and the breakdown of protein, respectively. Uric acid, on the other hand, is a metabolic product of purine depredation. In a healthy kidney, these key indicators are effectively filtered and excreted through urine(Lin, 2023). When renal function is impaired, their clearance is reduced, leading to elevated levels in the blood.

Nutraceuticals, often referred as medicinal plants, have long been recognized as an essential part of traditional healing practices. These plants have been used for centuries to prevent and treat various ailments and remain highly valued in complementary health system. Several studies have shown biological effects of phytomedicine, including anti-inflammatory, anti-tumor, and antimicrobial activities, largely attributed to the presence of unique bioactive compounds, including flavonoids, tannins, and various aromatic constituents. Most phytomedicine have shown impressive *in-vitro* activities but low *in-vivo* efficacy due to challenges associated related to bioavailability. Most organic compounds found in phytomedicine have poor water solubility, lipophilicity, and inappropriate molecular size resulting in poor absorption and hence poor systemic availability. To overcome these limitations, recent advancements have focused on green nanosynthesis, where plant extracts are used to biologically synthesize metallic nanoparticles in an environmental friendly manner. These nanoparticles, can act as a highly effective carriers, enabling targeted and sustained drug delivery, improving the stability and absorption of phytocompounds, and ultimately enhancing their therapeutic potential (Gunasekaran et al., 2014). In this study we observed that treatment with *M. oleifera* and MO-AgNPs effectively reduced elevated biochemical markers and helped restore normal functions of liver and kidney functions. Notably, the MO-AgNPs demonstrated excellent recovery compared to the crude extract. *M.oliefera* significantly lowers the concentration of renal and hepatic biomarkers, including ALT, AST, bilirubin, creatinine, and uric acid, but the recovery was significantly lower than

observed in MO-AgNPs at 4 mg/kg body weight. Silymarin treated group showed recovery; however, the extent of improvement was comparatively lower than observed in the other treatment groups. These findings are consistent with previous studies reporting the enhanced activity of greenly synthesized nanoparticles and hepatoprotective and nephroprotective properties of *Moringa oleifera* leaf extract, further supporting their role as natural antioxidant and cytoprotective agents.

Both the *Moringa oleifera* aqueous leaf extract and the greenly synthesized silver nanoparticles exhibited significant DPPH and hydroxyl radical scavenging activities. In both assays, the samples exhibited a concentration dependent increase in radical scavenging activity, indicating their ability to neutralize different types of reactive oxygen species, ultimately protecting the organs from oxidative damage. The synthesized Ag-NPs showed comparatively higher antioxidant activity than the crude plant extract in both DPPH and hydroxyl radical assays. This enhanced activity may be attributed to the presence of bioactive phytochemicals from *Moringa oleifera* that act as reducing and stabilizing agents during nanoparticles synthesis, thereby improving their radical scavenging ability.

Histoarchitectural evaluation is essential for determine the extent of tissue toxicity following exposure to chemical insults. It forms the basis for most clinical generalizations following diagnosis. Furthermore, it is practically impossible to substantiate biochemical and molecular findings in both clinical and experimental studies without supporting histological evidence.

In our study, CCl_4 administration in positive control group disrupted the histoarchitectural framework of the liver and kidney, causing severe vacuolation, macro vesicular steatosis, ballooning degeneration, cytoplasmic rarefraction, and compression of sinusoidal spaces. Treatment with *M. oleifera* and MO-AgNPs both demonstrated notable improvement; however, the extent of recovery was nearly restored to normal in the group treated with MO-AgNPs at 4 mg/kg body weight. Silymarin also showed better recovery though its effects were comparatively lower than those observed in the *M. oleifera* and MO-AgNPs treated groups, highlighting the enhanced therapeutic potential of *M. oleifera* against CCl_4 liver injury.

Administration of CCl_4 induces several histoarhitectural changes, including destruction of Bowman's capsule, severe epithelial desquamation, glomerular and tubular degeneration, and vascular congestion. In our study, MO-AgNPs at 4 mg/kg body weight produces near-complete restoration of the normal renal histoarchitecture. The *M. oleifera* crude extract at 500mg/kg body weight also promoted substantial recovery, with only mild desquamation and slight congestion in observed in renal tubules. In-contrast silymarin-treated group showed a mild impairment, while severe epithelial desquamation, damaged Bowman's capsule, glomerular and tubular degeneration, and congestion remained evident.

Although these findings demonstrate strong protective potential, certain limitations should be acknowledged. The study was conducted in an acute animal model, which may not fully represent chronic human hepatorenal diseases, limiting direct clinical translation. Additionally, molecular mechanisms such as gene expression, inflammatory cytokines, and signaling pathways were not explored, which could have provided deeper mechanistic insight. Long term toxicity, biodistribution, and pharmacokinetic behaviors of MO-AgNPs were also

not evaluated which are essential for assessing safety and translation potential. Furthermore, nanoparticles stability under physiological conditions was not extensively studied, and variability in phytochemical composition of *Moringa oleifera*due to environmental and processing factors may influence reproducibility of results. Importantly, although green synthesis of AgNPs reduced cytotoxicity due to phytochemical capping, previous studies have reported potential dose-dependent neurotoxic effects, including alteration in neurotransmitter levels and neural ultrastructure; thereby subtle organ-specific toxicity of Ag-NPs at higher doses or prolonged exposure can't be completely excluded and warrant further investigations.

In conclusion, it was determined that *M. oleifera* and its green synthesized silver nanoparticles exert strong hepatorenal effects against CCl_4 toxicity, with MO-AgNPs showing superior therapeutical potential. These findings highlight the promise of plants-based nanomedicine as an effective strategy for enhancing bioavailability and improving the clinical utility of phototherapeutics.

Ethical Approval: All experimental procedures involving lab animals were conducted in accordance with the ethical standards of the Department of Veterinary Pathology, Faculty of Veterinary an Animal Sciences, PMAS-Arid Agriculture University, Rawalpindi, and were approved by the university ethical committee. All efforts were made to minimize animal suffering and to reduce the number of animals used in the study.

Data Availability: The data sets generated and/or analyzed during the current study are included in published article and its supplementary information files. Further data supporting the findings of this study are available from the corresponding author upon reasonable request.

Conflict of Interest: The authors declare that they have no conflicts of interest related to this study.

Funding Statement: The author(s) received no financial support for the research, authorship, and/or publication of this research paper

Consent to publish declaration: Not Applicable

Competing interest: Not Applicable

Consent to Participate declaration: Not applicable

References:

ABDEL FATTAH, M. E., SOBHY, H. M., REDA, A. & ABDELRAZEK, H. M. 2020. Hepatoprotective effect of Moringa oleifera leaves aquatic extract against lead acetate–induced liver injury in male Wistar rats. *Environmental Science and Pollution Research,* 27**,** 43028-43043.

ASIF, M., YASMIN, R., ASIF, R., AMBREEN, A., MUSTAFA, M. & UMBREEN, S. 2022. Green synthesis of silver nanoparticles (AgNPs), structural characterization, and their antibacterial potential. *Dose-response,* 20**,** 15593258221088709.

ATTAH, A. F., AKINDELE, O. O., NNAMANI, P. O., JONAH, U. J., SONIBARE, M. A. & MOODY, J. O. 2022. Moringa oleifera seed at the interface of food and medicine: Effect of extracts on some reproductive parameters, hepatic and renal histology. *Frontiers in Pharmacology,* 13**,** 816498.

BANCROFT, J. D. & GAMBLE, M. 2008. *Theory and practice of histological techniques*, Elsevier health sciences.

BJÖRNSSON, H. K. & BJÖRNSSON, E. 2022. Drug-induced liver injury: Pathogenesis, epidemiology, clinical features, and practical management. *European journal of internal medicine,* 97**,** 26-31.

CHANG, Z., QIU, J., WANG, K., LIU, X., FAN, L., LIU, X., ZHAO, Y. & ZHANG, Y. 2023. The relationship between co-exposure to multiple heavy metals and liver damage. *Journal of Trace Elements in Medicine and Biology,* 77**,** 127128.

CHIȘ, A., NOUBISSI, P. A., POP, O.-L., MUREȘAN, C. I., FOKAM TAGNE, M. A., KAMGANG, R., FODOR, A., SITAR-TĂUT, A.-V., COZMA, A. & ORĂȘAN, O. H. 2023. Bioactive compounds in Moringa oleifera: mechanisms of action, focus on their anti-inflammatory properties. *Plants,* 13**,** 20.

GHIUȚĂ, I. & CRISTEA, D. 2020. Silver nanoparticles for delivery purposes. *Nanoengineered biomaterials for advanced drug delivery.* Elsevier.

GUNASEKARAN, T., HAILE, T., NIGUSSE, T. & DHANARAJU, M. D. 2014. Nanotechnology: an effective tool for enhancing bioavailability and bioactivity of phytomedicine. *Asian Pacific journal of tropical biomedicine,* 4**,** S1-S7.

HE, S., ZHAO, W., CHEN, X., LI, J., ZHANG, L. & JIN, H. 2022. Ameliorative effects of peptide phe-leu-ala-pro on acute liver and kidney injury caused by CCl4 via attenuation of oxidative stress and inflammation. *ACS omega,* 7**,** 44796-44803.

IMTARA, H., AL-WAILI, N., ABOULGHAZI, A., ABDELLAOUI, A., AL-WAILI, T. & LYOUSSI, B. 2021. Chemical composition and antioxidant content of Thymus vulgaris honey and Origanum vulgare essential oil; their effect on carbon tetrachloride-induced toxicity. *Veterinary World,* 14**,** 292.

IRUM SHEHZADI, I. S., SHAH, N., KHAN, M., SHUAIB, M., MUZAMMIL SHAH, M. S., KHAN, A., ALI, H., YASIR ANWAR, Y. A., FIRASAT HUSSAIN, F. H. & HAYAT KHAN, H. K. 2020. In vivo antioxidant potential of Raphanus sativus seeds in rat kidney against CCl4-induced toxicity.

JURAEV, A. & SHODIYEVA, E. 2026. Biochemical Roles of Liver Enzymes in Hepatocellular Injury and Cholestasis. *Journal of Clinical and Biomedical Research,* 2**,** 167-172.

KHAN, M. R. & ZEHRA, H. 2013. Amelioration of CCl4-induced nephrotoxicity by Oxalis corniculata in rat. *Experimental and toxicologic pathology,* 65**,** 327-334.

LAKSHMANAN, M. 2019. Drug metabolism. *Introduction to basics of pharmacology and toxicology: volume 1: general and molecular pharmacology: principles of drug action.* Springer.

LANG, T., LIPP, A.-M. & WECHSELBERGER, C. 2025. Xenobiotic toxicants and particulate matter: effects, mechanisms, impacts on human health, and mitigation strategies. *Journal of Xenobiotics,* 15**,** 131.

LIN, W. 2023. Clinical significance of serum creatinine, urea nitrogen and uric acid levels in patients with chronic renal failure. *International Journal of Biology and Life Sciences,* 3**,** 19-26.

MAGALHÃES, A. F. A. & CALDAS, E. D. 2019. Occupational exposure and poisoning by chemical products in the Federal District. *Revista Brasileira de Enfermagem,* 72**,** 32-40.

MOHAMMED, G. M. & HAWAR, S. N. 2022. Green biosynthesis of silver nanoparticles from Moringa oleifera leaves and its antimicrobial and cytotoxicity activities. *International Journal of Biomaterials,* 2022**,** 4136641.

MUKKAVALLI, S., CHALIVENDRA, V. & SINGH, B. R. 2017. Physico-chemical analysis of herbally prepared silver nanoparticles and its potential as a drug bioenhancer. *OpenNano,* 2**,** 19-27.

NURHAYATI, T., RIDHO, M. F., SANTOSO, P. T. R., SETIAWAN, S., GOENAWAN, H. & TARAWAN, V. M. 2024. Effects of Moringa oleifera leaf extract on liver histopathology: a systematic review. *Journal of Nutrition and Metabolism,* 2024**,** 6815993.

PATEL, S., CHOPRA, S., CHAURASIA, S. & SARWAT, M. 2022. Plant based bioavailability enhancers. *Current Pharmaceutical Design,* 28**,** 642-654.

POP, O. L., KEREZSI, A. D. & CIONT, C. 2022. A comprehensive review of Moringa oleifera bioactive compounds—cytotoxicity evaluation and their encapsulation. *Foods,* 11**,** 3787.
RAMÍREZ-MEJÍA, M. M., CASTILLO-CASTAÑEDA, S. M., PAL, S. C., QI, X. & MÉNDEZ-SÁNCHEZ, N. 2024. The multifaceted role of bilirubin in liver disease: a literature review. *Journal of Clinical and Translational Hepatology,* 12**,** 939.
SHABAN, N. S., ABDOU, K. A. & HASSAN, N. E.-H. Y. 2016. Impact of toxic heavy metals and pesticide residues in herbal products. *Beni-suef university journal of basic and applied sciences,* 5**,** 102-106.
SHEHZADI, I., SHAH, N. A., KHAN, M. R., SHUAIB, M., SHAH, M., KHAN, A., ALI, H. S. M., ANWAR, Y., HUSSAIN, F. & KHAN, H. 2019. In vivo antioxidant potential of raphanus sativus seeds in rat kidney against CCl4-induced toxicity. *Polish Journal of Environmental Studies,* 29**,** 277-284.
STANLEY, L. 2024. Drug metabolism. *Pharmacognosy.* Elsevier.
SWETHA, M., RADHA, C. & MUTHUKUMAR, S. 2018. Bioaccessibility and bioavailability of Moringa oleifera seed flour polyphenols. *Journal of Food Measurement and Characterization,* 12**,** 1917-1926.
ULLAH, H., KHAN, A., BAIG, M. W., ULLAH, N., AHMED, N., TIPU, M. K., ALI, H. & KHAN, S. 2020. Poncirin attenuates CCL4-induced liver injury through inhibition of oxidative stress and inflammatory cytokines in mice. *BMC complementary medicine and therapies,* 20**,** 115.
UNSAL, V., CICEK, M. & SABANCILAR, İ. 2021. Toxicity of carbon tetrachloride, free radicals and role of antioxidants. *Reviews on environmental health,* 36**,** 279-295.
WIDATALLA, H. A., YASSIN, L. F., ALRASHEID, A. A., AHMED, S. A. R., WIDDATALLAH, M. O., ELTILIB, S. H. & MOHAMED, A. A. 2022. Green synthesis of silver nanoparticles using green tea leaf extract, characterization and evaluation of antimicrobial activity. *Nanoscale Advances,* 4**,** 911-915.
ZARGAR, S. & WANI, T. A. 2021. Protective role of quercetin in carbon tetrachloride induced toxicity in rat brain: biochemical, spectrophotometric assays and computational approach. *Molecules,* 26**,** 7526.
ZHANG, S., REN, H.-F., DU, R.-X., SUN, W.-L., FU, M.-L. & ZHANG, X.-C. 2023. Global, regional, and national burden of kidney dysfunction from 1990 to 2019: a systematic analysis from the global burden of disease study 2019. *BMC Public Health,* 23**,** 1218.

Supplementary Files

This is a list of supplementary files associated with this preprint. Click to download.

- UsamaAbbasi20240917tab1.docx
- GraphicalAbstractppt.pptx
- Histopathology.docx
- RFT.docx